Διπλωματική Εργασία

Υδροδυναμικά μεγέθη εντός ύφαλου ομογενούς κυματοθραύστη

Παναγιώτα Μίγγου

Ιούλιος 2011

Delft University of Technology

Master Thesis Report

Wave kinematics inside homogeneous submerged rubble-mound breakwater

Panagiota Mingou

July 2011

COLOPHON

MSc thesis report
Title: “Wave kinematics inside homogeneous rubble-mound submerged breakwater”

Author
Panagiota I. Mingou
panagiota.mingou@gmail.com

Institutes
Technical University of Delft
National Technical University of Athens (NTUA)

Graduation committee

Prof. Drs. Ir. Constantine Memos	Hydraulic Engineering, NTUA
Ir. H.J. Verhagen	Hydraulic Engineering, TU Delft
Drs.Ir. Papanikolaou	Hydraulic Engineering, NTUA
Drs. Ir. Tsoukala	Hydraulic Engineering, NTUA

PREFACE

This master thesis is written as a final part of my studies for the diploma of Civil Engineering at National Technical University of Athens (NTUA). This graduation project took place at Delft University of Technology in the framework of ERASMUS student exchange program I participated in.

Executing a graduation project is an integral part of the education program at Civil Engineering and is regarded as the final work of the education in which the student shows his skills and knowledge obtained at the faculty. The focus of this project was on water circulation inside breakwaters and a major part of the research was executed by experiments in the wave flume of the Stevin III-laboratory at Delft University. The topic of breakwaters is a part of the Coastal Engineering section; however, the laboratory is a part of the Fluid Mechanics section.

This report is an overview of an investigation on the thesis subject: Sufficiency of new water for marine life inside homogenous submerged rubble-mound breakwater. The main research objective is to obtain a proper insight of the water flow inside breakwater and to define a method to predict the adequacy of new water for the prospective inhabitants of the breakwater. For the investigation of this subject, a physical model was developed at the Laboratory of Fluid Mechanics of TU Delft.

I would like to thank in the first place prof. H.J. Verhagen (from TU Delft) for his instrumental arrangements and thoughtful supervision. I am equally thankful to prof. C. Memos (from NTUA) for providing me this opportunity and sharing his knowledge. I am also grateful to S. de Vree for his daily technical support during tests.

P. Mingou
Athens, July 2011

ABSTRACT

The main objective of this study is to give estimation about the pore velocity of a homogenous rubble-mound submerged breakwater as well as the flow of water inside it for different water levels. This research has been performed by means of a physical model. Five variables are considered in this study:

- wave period
- wave height
- submergence factor
- pore velocity
- pressure differences

Also, some consideration was given on the environmental impact of a homogenous rubble-mound breakwater. It would be interesting to investigate whether with given conditions marine life could inhabit in the breakwater.

In the analysis of the data collected from the measurements, the impact of the varying parameters is investigated leading to useful conclusions and better understanding of the entire process.

Finally, suggestions of further research on this topic are discussed.

KEYWORDS

Submerged
Rubble mound
Homogenous
Breakwater
Pore velocity
Water flow
Pressure gradient

ΕΚΤΕΝΗΣ ΠΕΡΙΛΗΨΗ

Οι κυματοθραύστες αποτελούν σημαντικό παράγοντα για την διατήρηση και ανάδειξη των παράκτιων περιοχών, εξαιτίας της μεγάλης συγκέντρωσης πληθυσμό σε αυτές. Όσον αφορά τους ύφαλους κυματοθραύστες, παρουσιάζουν σημαντικά πλεονεκτήματα σε σχέση με τους ύφαλους, όπως η οικονομικότερη κατασκευή και συντήρηση, η πιο ήπια παρέμβαση στο αισθητικό περιβάλλον και η διατήρηση θαλάσσιας ζωής στο εσωτερικό τους. Η θαλάσσια χλωρίδα και πανίδα έλκεται από τους φυσικούς ογκολίθους για τροφή και προστασία. Είναι σημαντικό λοιπόν να μελετηθεί εάν υπάρχει επαρκής ανανέωση νερού και άρα οξυγόνου στο εσωτερικό μιας τέτοιας κατασκευής ώστε να μπορέσει να φιλοξενήσει ζώα και φυτά της θάλασσας.

Η επιλογή της τυπικής διατομής του κυματοθραύστη που θα μελετηθεί για το σκοπό αυτό επιλέχθηκε ώστε να ανταποκρίνεται σε πληθώρα περιπτώσεων. Έτσι, παραλήφθηκε ο πυρήνας και άλλα υποστρώματα και έτσι η κατασκευή προέκυψε ομογενής, πράγμα που διευκολύνει και την ανανέωση των υδάτων και άρα το σκοπό αυτής της μελέτης. Η ευστάθεια του κυματοθραύστη μελετήθηκε με βάση το τυπικό κύμα σχεδιασμού για τα δεδομένα της Μεσογείου και έτσι προέκυψε το μέγεθος των ογκολίθων που αποτελούν την κατασκευή.

Το εύρος των τιμών που επιλέχθηκε για τα πειράματα είναι 0,40-1,40μ ύψη κύματος, δηλαδή για μικρά σχετικά κύματα που εμφανίζονται κυρίως κατά την καλοκαιρινή περίοδο και απέχουν κατά πολύ από το κύμα σχεδιασμού. Αυτό συνέβη για να μελετηθεί η ανανέωση των υδάτων για τη δυσμενέστερη περίπτωση, δηλαδή για την περίπτωση κυμάτων μικρού ύψους. Μελετήθηκαν σενάρια για διάφορους συνδυασμούς υψών και περιόδων κύματος, ενώ τα σενάρια αυτά επαναλήφθηκαν για διαφορετικούς συντελεστές βύθισης ώστε να κατανοηθεί και η επιρροή αυτής της παραμέτρου στην έρευνα αυτή.

Σε πειραματικό μοντέλο υπό κλίμακα τοποθετήθηκαν ταχύμετρα και πιεσόμετρα για να προσδιοριστεί η ανανέωση των υδάτων στο εσωτερικό του ύφαλου ομογενούς κυματοθραύστη. Τοποθετήθηκαν στο μισό του ύψους της κατασκευής H/2 ενώ κατά μήκος αφού χωρίσαμε την κατασκευή σε τρία μέρη, ανάντη πρανές, στέψη και κατάντη πρανές, τοποθετήσαμε ένα ταχύμετρο σε κάθε μέρος. Τα σενάρια για διαφορετικά ύψη και περίοδοι κύματος καθώς και για συντελεστές βύθισης τροποποιήθηκαν σε κλίμακα ώστε να προσομοιάζουν τις καταστάσεις σε φυσική κλίμακα.

Κατά την ανάλυση των πειραματικών δεδομένων μελετήθηκε η επιρροή του ύψους κύματος και της διαμέτρου των ογκολίθων στις ταχύτητες στο εσωτερικό του κυματοθραύστη για διαφορετικούς συντελεστές βύθισης. Στη συνέχεια, μελετήθηκε η επιρροή της περιόδου των κυματισμών στις ταχύτητες για διαφορετικούς συντελεστές βύθισης. Επίσης, με βάση τα πειράματα μελετήθηκε η σχέση μεταξύ των ταχυτήτων ανάντη και εντός του κυματοθραύστη ενώ προέκυψε ότι οι διαφορικές πιέσεις συνδέονται με τις

ταχύτητες μέσω της εξίσωσης Bernoulli για δεδομένη διαπερατότητα του υλικού που χρησιμοποιήθηκε. Καθώς αναλύθηκε η επιρροή των διαφορικών πιέσεων για διαφορετικά ύψη και περιόδους κύματος και για διαφορετικούς συντελεστές βύθισης, προέκυψε ότι ο μηχανισμός των διαφορικών πιέσεων είναι διαφορετικός για το πρώτο και το δεύτερο μισό του κυματοθραύστη.

Τα βασικότερα συμπεράσματα που προέκυψαν από την μελέτη αυτή παρουσιάζονται παρακάτω. Φαίνεται καθαρά ότι οι μικρότερες ταχύτητες στο εσωτερικό του κυματοθραύστη εμφανίζονται στο μέσο του, ενώ οι ταχύτητες γενικά μειώνονται για αύξηση του συντελεστή βύθισης. Οι ταχύτητες ανάντη του κυματοθραύστη είναι πάντοτε μεγαλύτερες σε σχέση με αυτές στο εσωτερικό της κατασκευής, λόγω της διαφοράς διαπερατότητας των δυο μέσο αλλά και λόγω της ροής νερού επάνω από τον κυματοθραύστη για συντελεστές βύθισης μεγαλύτερες του μηδενός. Ο λόγος των διαφορικών πιέσεων μεταξύ του δεύτερου και του πρώτου μισού της κατασκευής είναι ανεξάρτητες από το ύψος και την περίοδο του κύματος ενώ ο λόγος αυτός μειώνεται για μεγαλύτερους συντελεστές βύθισης. Σε κάθε περίπτωση οι διαφορικές πιέσεις στο πρώτο μισό του κυματοθραύστη είναι μεγαλύτερες σε σχέση με αυτές στο δεύτερο μισό της κατασκευής.

Οι κυριότερες προτάσεις για περεταίρω μελέτη παρουσιάζονται παρακάτω. Περεταίρω διερεύνηση των παραμέτρων που λήφθηκαν υπόψη σε αυτήν την μελέτη. Για παράδειγμα, μεγαλύτερο εύρος τιμών για ύψη και περιόδους κύματος καθώς και για συντελεστές βύθισης. Επιπλέον μπορούν να εισαχθούν παραπάνω παράμετροι που αφορούν το αντικείμενο αυτό και παραλήφθηκαν χάριν απλοποίηση όπως το μήκος της στέψης, η κλίση των πρανών και η επιρροή του ανέμου.

Table of contents

List of symbols

A	amplitude	[m]
a	Forchheimer coefficient	[s/m]
B	crest width	[m]
b	Forchheimer coefficient	[s^2/m^2]
c	Forchheimer coefficient	[-]
C_t	transmission coefficient	[-]
C_r	reflection coefficient	[-]
d	water depth	[m]
D_{n50}	nominal stone diameter	[m]
D_{n50A}	nominal stone diameter of armour layer	[m]
D_{n50F}	nominal stone diameter of filter	[m]
D_{n50C}	nominal stone diameter of core	[m]
D_{15}	15% value of sieve curve	[m]
D_{50}	sieve diameter, diameter of stone that exceeds the 50% value of the sieve curve	[m]
D_{85}	15% value of sieve curve	[m]
g	gravity acceleration	[m/sec^2]
H	structure height	[m]
h	wave height	[m]
h_t	transmitted wave height	[m]
h_r	reflected wave height	[m]
h_i	height of water column (Bernoulli)	[m]
Δh_{ij}	height difference of water column (Bernoulli)	[m]
h_s	significant wave height	[m]
i	pressure gradient	[-]
k	permeability	

K	wave number	
L	wave length	[m]
L'	wave length inside the breakwater	[m]
L_a	distance between two velocity meters	[m]
L_b	distance between two velocity meters	[m]
L_0	deep-water eave length	[m]
M_{15}	mass of particle for which 15% of granular material is lighter	[kg]
M_{50}	mass of particle for which 50% of granular material is lighter	[kg]
M_{85}	mass of particle for which 85% of granular material is lighter	[kg]
N_s^*	Stability spectral number	[-]
P	notional permeability	[-]
P_i	pressure	[Pa]
ΔP_a	pressure difference at the front face	[Pa]
ΔP_b	pressure difference at the back face	[Pa]
p_{max}	maximum subsurface pressure across the breakwater	[Pa]
p	subsurface pressure	[Pa]
n	porosity	[-]
S	Damage level	[-]
s	wave steepness	[-]
T	wave period	[sec]
T_s	significant wave period	[sec]
sf	submergence factor	[-]
u	horizontal particle velocity	[m/sec]
v	real velocity	[m/sec]
v_1	real velocity measured at the front of the breakwater	[m/sec]
v_2	real velocity measured in the middle of the breakwater	[m/sec]
v_3	real velocity measured at the back of the breakwater	[m/sec]
v_f	filter velocity	[m/sec]
w	vertical particle velocity	[m/sec]
z	vertical distance from SWL	[m]

z_1	freeboard crest zone	[m]
z_2	structure zone	[m]

List of Greek symbols

α	Forchheimer coefficient	
β	Forchheimer coefficient	
γ_f	roughness reduction factor	
γ	specific weight	[kg/m^3]
δ	damping coefficient	[-]
ρ	material density	[kg/m^3]
ρ_w	water density	[kg/m^3]
ω	circular frequency	

LIST OF FIGURES, TABLES AND PICTURES

1 INTRODUCTION

Coastal areas are home to a large and growing proportion of the world's population. The high concentration of people in coastal regions has produced many economic benefits, including improved transportation links, industrial and urban development, revenue from tourism, and food production. Great attention to stability and sustainable development of the coastal zone is therefore paid by government authorities, coastal managers, owners of real estate and many other stakeholders. Offshore breakwaters are one of the most professional engineering measures often chosen for the sake of shaping shores, from among a variety of coastal protection structures.

Most ancient coastal efforts were directed to port structures, with the exception of a few places where life depended on coastline protection. Venice and its lagoon is one such case. Protection of the shore in the Netherlands, Italy and England can be traced back at least to the 6th century. In ancient times phenomena such as the Mediterranean currents and wind patterns and the wind-wave cause-effect link were completely understood.

1.1. Breakwaters

Breakwaters are structures constructed on coasts as part of coastal defense or to protect an anchorage from the effects of weather and longshore drift. The material used for their construction can be natural or artificial stone (e.g. tetra pod) or caissons. The functioning of breakwaters depends on their geometrical dimensions (1) in relation to the external hydraulic forcing, (2) local sediment transport and (3) morphodynamics. Their primary function is to reduce wave energy at the shoreline by modifying waves and currents. Breakwaters can also redistribute sediment transport patterns so as to improve beach features, provide toe support for perched beaches and even shelter harbours or prevent siltation in port approach channels.

Primary distinction must be made between sheltering harbours and coastal protection ones. Coastal protection breakwaters can be submerged or emerged while harbour breakwaters are usually emerged.

1.1.1. Submerged breakwaters

Submerged breakwaters have a rather secondary effect on wave propagation but can generally cause transformation of waves and currents. The most important function of this kind of breakwater would be to protect the beach against waves and thus improve the wave climate in the area.

In addition, it can be noted that the submerged breakwater has two energy dissipation mechanisms that attenuate wave height. First, energy is dissipated when the wave breaks due to the abrupt change in water depth as it meets the front face of the submerged breakwater. Secondly, energy dissipation takes place on the surface and in the permeable layer of the submerged breakwater.

1.1.1.1. Classification of submerged breakwaters

Low-crested structures can be classified into three categories: dynamically stable reef breakwaters, statically stable low-crested structures with the crest above SWL and statically stable submerged structures.

Dynamically stable reef breakwaters (Figure 1.1)

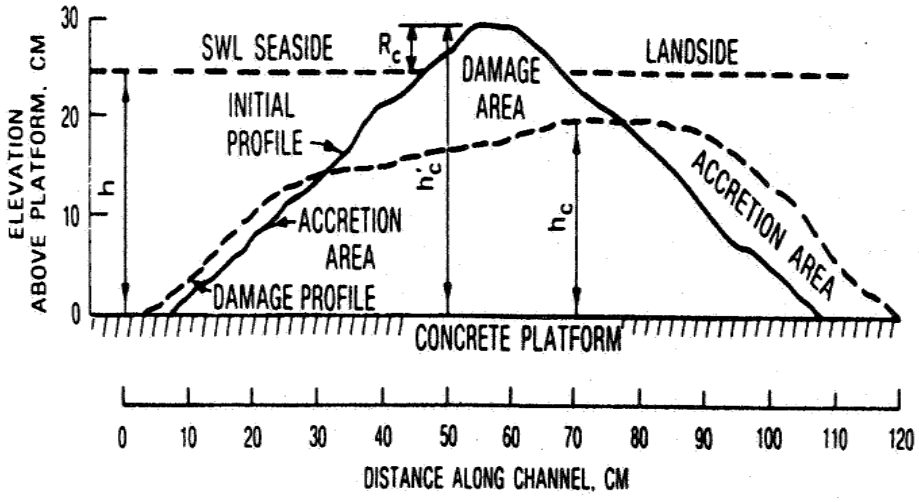

Figure 1.1 Dynamically stable reef breakwaters from Van der Meer journal [1993]

A reef breakwater is a homogenous pile of stones without filter layer or core and it is allowed to reshape by wave attack. The equilibrium crest height, with corresponding transmission is the main design parameters.

This type of breakwater is a little more than a homogenous pile of stones with individual stone weight similar to those ordinarily used in the armour and/or the first underlayer of conventional breakwaters. The initial crest height is just above the water level. Under severe wave condition it is allowed that the crest height decreases to a certain equilibrium crest height. This equilibrium crest height and corresponding transmission are the main design parameters. It is clear that the larger the crest freeboard R_c gets the less efficient the submerged breakwater becomes.

The idea behind such reef breakwater is that its form changes due to wave attack. Due to its rather large permeability, the reef breakwater type is not very well suited for supporting the toe of a beach fill since the sand will move through the breakwater too easily.

Clear cut demarcation lines between submerged breakwaters and sills (or reefs) have not yet been established but it might be assumed that the former have a height h_B of more than 40-50% of water depth h, or the relative submersion (freeboard) $(h- h_{B)}/h_{B<}0.5$, while the latter are lower.

Statically stable submerged breakwaters (Figure 1.2)

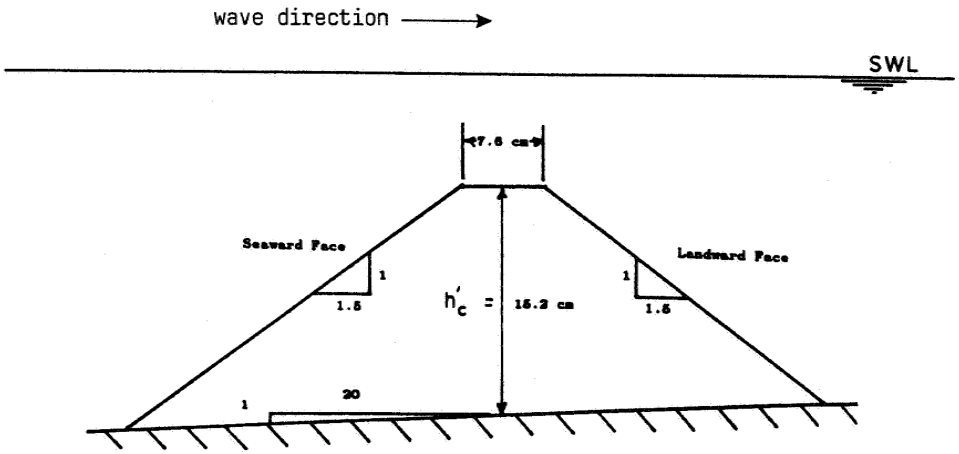

Figure 1.2 Statically stable submerged breakwaters from Van der Meer journal [1993]

All waves overtop these structures and the stability increases remarkably if the crest height decreases. It is obvious that wave transmission is substantial at these structures.

In recent years a new concept of tandem breakwaters emerged, which employs a submerged reef breakwater in front of a main surface-piercing structure to protect the latter from severe waves. The submerged reef breakwater serves to reflect and dissipate wave energy, thereby reducing the intensity of wave action on the main structure, which can then be designed with more economic materials. It is clear that the larger the crest freeboard R_c gets the less efficient the submerged breakwater becomes.

1.1.1.2. Advantages and disadvantages of submerged breakwaters

Offshore, submerged porous reefs respond to the growing demand for environmental friendly solutions to coastal protection. They can achieve this by unifying coastal protection, environmental effects, and aesthetic advantage into a multi-functional structure. Thus, they are needed because other coastal protection solutions do not offer the same overall value to the community.

Submerged breakwaters can have a lot more advantages compared to emerging ones, depending on the purpose of the breakwater.

1. First of all, submerged breakwaters can sustain habitants. So they can help protect and sustain the marine environment.
2. Submerged breakwaters have a relatively mild but steady effect in retaining shore side sediment and have a milder effect on the surrounding coast. Therefore submerged breakwaters are recently replacing emerging breakwaters in many places of the world.
3. Water exchange behind submerged breakwaters is better than that for the emerging ones. Thus, stagnant water can be avoided.
4. Submerged breakwaters may be foreseen as long continuous structures (thus avoiding gaps and drawbacks connected with them).
5. Sometimes, submerged breakwaters can dissipate wave energy more efficiently than emerging ones due to the fact that in emerging breakwaters longshore transport can be interrupted by the growing salient or even a tombolo.
6. They do not spoil the aesthetic aspect of the beach.
7. The advantages include preservation of environment and relatively low capital investments.

Last but not least, one should not neglect some disadvantages of submerged breakwaters.

1. They may become fatal obstacles for fishing boats or small pleasure boats
2. The effect of a submerged breakwater on a coast with a wide tidal range is not obvious because the hydraulic function of the submerged breakwater depends of the water depth at the crown, especially at tidal coasts.
3. The reef may be difficult to inspect since it is underwater.
4. It may be difficult and expensive to build the reef because it is both offshore and submerged. Construction requires a floating plant and thus may be expensive.

1.2. Problem definition and research objectives

From an environmental point of view, breakwaters can be used not only to improve the wave climate, but also to maintain marine life inside them. It is very common that fish are attracted to natural rock for shelter and food. This way, constructing a homogenous rubble mound breakwater with high porosity would appeal a lot to marine flora and fauna. The objective behind the concept is to see if such a breakwater could maintain life and promote the diversity and abundance of it, while at the same time performing its technical function as coastal protection.

The goal of this thesis is a natural consequence of the problem definition: to acquire knowledge about whether a homogenous rubble-mound submerged breakwater can sustain marine life. Standard water refreshment is essential for marine inhabitants under all conditions. From the biologic point of view the basic parameters that can give information about whether a mean can sustain marine life inside it is measuring the pressure difference inside the breakwater for different wave conditions. Also, it would be interesting if we get estimation about velocities inside such a breakwater and how they vary for different occasions.

Different wave heights and steepnesses are tested. Of course, it is not interesting to investigate waves close to design, but to relatively small ones in order to see if sufficient water flow is acquired for low wave heights. Also it is very important to see how the submergence of the breakwater affects the flow and the velocities inside it. It is also important to get estimation about wave and generally energy damping, or transmission of submerged breakwaters.

Regarding the fact that flow and velocity inside a breakwater can be a multi-parametric process, the problem is approached empirically and not analytically. To reach these objectives, research objective will be investigated with a physical model in a wave flume of the Fluid Mechanics Laboratory of the Delft University of Technology.

Summarized: *'The goal of this master thesis is to describe the flow and the velocities occurred inside a homogenous submerged rubble-mound breakwater, the final objective being to combine technical and environmental points of view. The influence of the most relevant parameters in this process is explored.'*

1.3. Methodology

As stated in the title, the whole issue is approached experimentally. The steps followed in order to perform a complete research which will be able to draw safe conclusions are the following:

- First, a thorough study on the existing related literature is conducted in order to understand the basis of the problem and identify the critical parameters that should be taken into consideration.
- The second step is the design of a proper scale model which will simulate as realistic as possible the relevant physical processes. Depending on the available equipment, the model should be able to reproduce all the dominant parameters. The experimental set-up requires also an accurate and handy measuring system.
- Next, a practical test procedure is defined and the experiment is executed. During this step, apart from the continuous monitoring and inspection of all the devices, a regular evaluation of the results is performed. This evaluation may lead to adjustments of the experiment plan.
- The forth step consists of the analysis of the results. The influence of the dominant parameters on the process is investigated and through analysis of these data, the development of a prediction method is attempted.
- Finally, the last stage is to draw conclusions, apply the proposed method and give some recommendations for further research.

1.4. Reader

This report begins in Chapter 2 with a study of relevant existing theories and studies about pore velocity and pressure gradients inside a breakwater. Chapter 3 describes several elements of the laboratory research. In Chapter 4 the analysis of the experiment results is described. The final conclusions and recommendations are given in Chapter 5.

2 LITERATURE REVIEW

Permeable coastal structures such as rubble mound breakwaters are of great interest in coastal and harbour engineering. These structures are capable of protecting a coastal area from excessive wave action by dissipating the incident wave energy. When studying the structural response of rubble mound breakwaters to wave loading, the knowledge of pore pressures and related wave attenuation inside the porous structure is important since the pore pressures affect most responses, such as wave run-up, wave overtopping, reflection, transmission and the hydraulic and geotechnical stability of the breakwater.

Furthermore, it is interesting to study the pore pressures and velocity inside the breakwater so that we can draw safe conclusions about whether it could maintain marine life or not.

2.1. Physical dimensions

In order to conduct a proper experimental research, it is essential that we first understand the way that the phenomena works. This includes previous work that has been done on this field and also some theoretical knowledge connected to it.

2.1.1. Crest height and submergence factor

The crest height of a structure is defined in terms of the crest freeboard (R_c). The crest freeboard is the vertical distance between the horizontal part of the crest and the SWL (still water level). In submerged breakwaters the crest height plays an important role in the technical function of the structure. This variation is usually given with a submergence factor. The crest elevation usually varies from -3m until 0m for submerged structures. Submergence factor is the ratio between the crest freeboard and the structure height and usually varies between 0 for structures in between submerged and emerging and 0.50 for deeply submerged breakwaters. Structures with submergence factor greater the 0.50 have almost no technical function.

It should also be stated here that the submergence of a breakwater is a function of the tidal range. That means that a submerged breakwater can be emerging when there is low tide or very deep submerged when the tide is high. The problems occurring from tides is that the function and characteristics of breakwater changes for the first situation while a breakwater with high submergence factor have no influence on the waves for the second one.

A distinction can be made within the two zones: zone z_1 which is practically the crest freeboard (R_c) and zone z_2 which is equal to the height of the structure (H). Now, the submergence factor can be defined,

$$sf = \frac{R_c}{H} = \frac{z_1}{z_2} \tag{2.1}$$

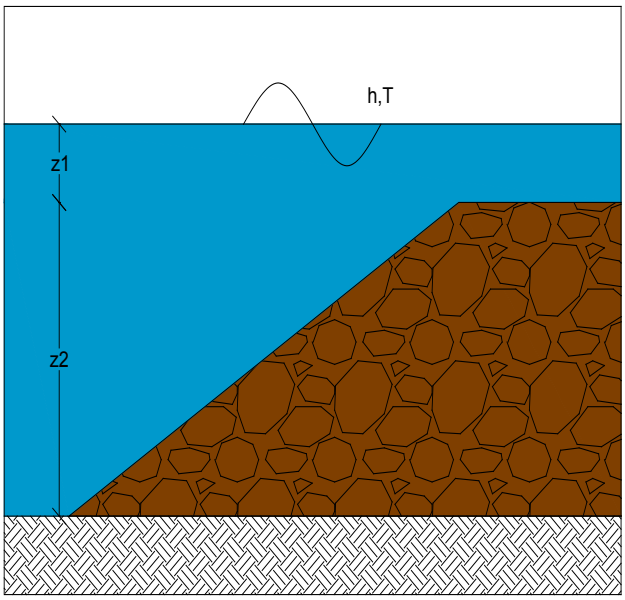

Figure 2.1 Figure of breakwater

2.1.2. Crest width

Concerning this parameter, submerged structures could be divided to narrow-crested and broad-crested ones. Narrow crested breakwaters are considered the structures for which B/h<10, while for wide structures it is B/h>10.

However, narrow crested structures become a lot less effective in high tidal states or when storms occur. On the other hand, broad-crested structures are more expensive and they should always be supported by proper cost-benefit studies. The rule of thumb for this parameter is that the wider the crest the more wave energy dissipation will occur (the lower the wave transmission). The crest width is usually close to the height of the structure mainly for stability purposes. Last but not least, interlocking, especially on the outer layer is as important as in non-overtopped breakwaters.

2.1.3. Slope

The slope angle has a large influence on submerged structures, but in this case wave attack is concentrated on the crest and less on the seaward slope. Therefore, it might be allowed to exclude the slope angle of submerged structures as being a governing parameter for stability or wave climate. Usually, slope angles in non-overtopped breakwaters vary from 1:3 to 1:1.5 behind the breakwater depending also on the size of the stones. If seismic activity is to be taken into account, the slopes should generally be gentler, to allow for the expected horizontal accelerations to be absorbed without damage. Also, it is not uncommon to see different slope angles in the seaward and landward face of the breakwaters. It shouldn't be neglected that slope angle and wave reflection are closely connected parameters. In fact, the steeper the slope is, the larger the wave reflection.

2.2. Material

In the case of a homogeneous rubble mound breakwater stone diameter and gradation are of utmost importance and they are mainly connected to stability variables. Also, stone placement and interlocking can also affect the functioning of the structure.

2.2.1. Porosity & permeability

Porosity (n) is defined as the percentage of voids between units or particles. This parameter mainly depends on the grading, shape and method of placement of the armour stones on the slope. Loose materials always have some porosity. For rock and concrete armour the porosity may range roughly between 30-55%.

$$n = \frac{V_V}{V_T} \tag{2.2}$$

The permeability of a structure mostly depends on the size of the rock layers. It is generally given as a notional index that represents the global permeability of the structure, or as the ratio of diameters of core material and armour material. Also, it influences armour stability, wave run-up and wave overtopping. Notional permeability is a parameter used in the van der Meer [1988] stability formula to make sure that the permeability of the structure is taken into account. It has no physical meaning and is experimentally defined. Usually it varies from 0.1 to 0.6.

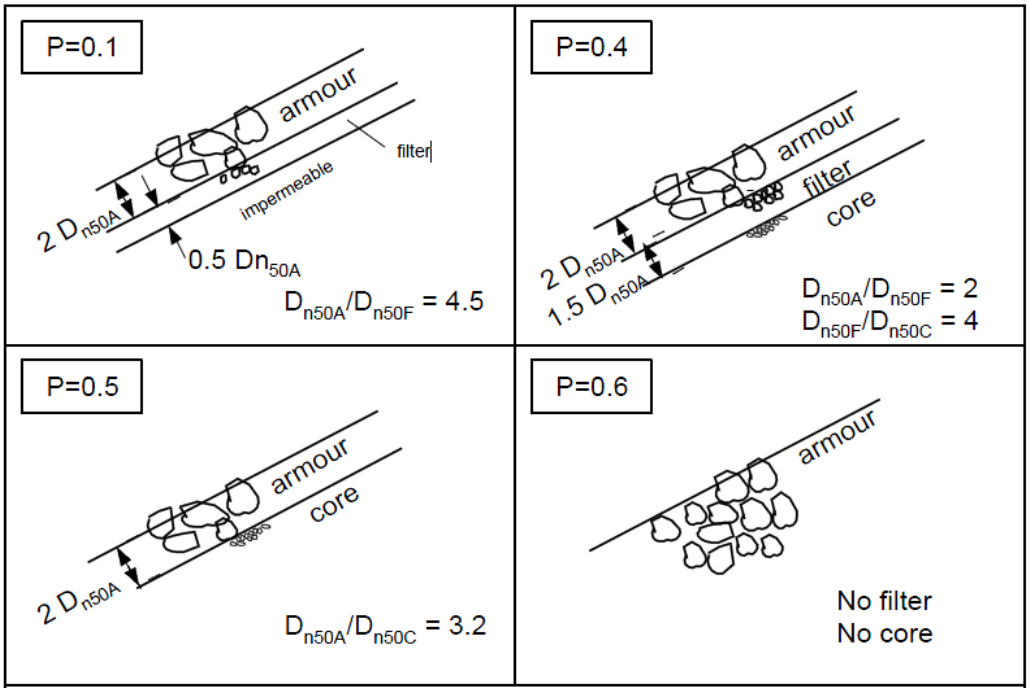

Figure 2.2 Notional permeability factor Van der Meer [1988]

2.2.2. Roughness

Roughness is created by irregular shaped block revetments, artificial ribs or blocks on a smooth slope. Generally, rubble mound and concrete block structures have the highest roughness factors. Values for roughness reduction factor γ_f can be found in The Rock Manual.

2.3. Hydraulic parameters

A wave is the generic term for any periodic fluctuation in water height, velocity or pressure. The term sea is often used for fresh waves, where the driving wind force is still active, in contrast to swell. Swell is the name for waves caused by wind but possibly long ago (days) and far away on the ocean (thousands of km), traveling on with the slowly dissipating, energy gained from the wind.

2.3.1. Wave height and wave period

The wave height is defined as the difference between the maximum and minimum elevations of the sea-surface over the duration of the wave. This duration is called the wave period in the time domain. The wave period is the time between two zero crossings.
In case of regular waves, it is not very difficult to determine the significant wave height h_s and the significant wave period T_s, because they are the same for all the waves. Consequently, there is just one correct value for both parameters.
In case of an irregular wave spectrum, breakwaters are commonly not designed with respect to one individual wave but are based on the characteristic values of sea-states. Therefore the incident wave height is usually given as the significant wave height.

2.3.2. Wave steepness and relative wave height

Wave steepness is defined as the ratio of wave height over wave length: s=h/L. This number can give some information about the wave's generation and characteristics. Generally a steepness of s=0.01 indicates a typical swell wave and a steepness of 0.04 to 0.06 a typical wind wave.

2.3.3. Wave length

The significant wave length (L) is equal to

$$L = \sqrt{gd}\left(1 + \frac{d}{L_0}\right)T \quad \text{for } \frac{d}{L_0} < 0.36 \tag{2.3a}$$

$$L = L_0 = \frac{g}{2\pi}T^2 \quad \text{for } \frac{d}{L_0} \geq 0.36 \tag{2.3b}$$

according to Visser's approximation. The wave flume in this research is considered as transitional water, so the formula for the wave length can also be applied.

2.3.4. Transmission and reflection

Transmission is defined as the wave energy that travels past the breakwater. The wave energy that is attenuated in the lee of the breakwater is either dissipated by the structure or reflected back as reflected wave energy. The effectiveness of a breakwater in attenuating wave energy can be measured by the amount of wave energy that is transmitted past the structure. The larger the wave transmission coefficient is, the less the wave attenuation. For submerged breakwaters, the larger the submergence is, the lesser wave energy will impact the structure, and so the structure becomes less effective for wave attenuation. Wave transmission is quantified by the use of the wave transmission coefficient

$$C_t = \frac{h_t}{h} \tag{2.4}$$

where h_t is the transmitted wave height and h the incident wave height. There are also numerous graphs of empirical data from wave tank tests that can be used to determine wave transmission coefficients.

Reflection in breakwaters is mainly a function of the material used and the slope angle. It is profound that for steeper slopes, bigger reflection occurs. Of course for submerged breakwaters, reflection can be literally zero as submergence factor increases. Wave reflection is quantified by the use of wave reflection coefficient

$$C_r = \frac{h_r}{h} \tag{2.5}$$

where h_r is the reflected wave height and h the incident wave height

2.4. Velocity inside submerged breakwater

Water in motion can be fully described by the Navier-Stokes equations, but in different situations, different terms can be neglected.

$$\frac{\partial u}{\partial t} + u\frac{\partial u}{\partial x} + w\frac{\partial u}{\partial z} = -\frac{1}{\rho}\frac{\partial p}{\partial x} + \upsilon\frac{\partial u}{\partial z^2} - \frac{\partial \overline{u'^2}}{\partial x} - \frac{\partial \overline{u'w'}}{\partial z} \tag{2.6}$$

In most coastal structures that contain a permeable part, wave action causes non-stationary flow. Derived from the Navier-Stokes equation the Forchheimer equation is valid for stationary flow. Polubarinova [1962] added a time dependent term. This formula is referred to as the extended Forchheimer equation:

$$\frac{1}{\rho g} = i = av_f + bv_f\left|v_f\right| + c\frac{\partial v_f}{\partial t} \tag{2.7}$$

where $a = \alpha\frac{(1-n)^2}{n^3}\frac{\upsilon}{gD_{n50}}$ and (2.8)

$b = \beta\frac{1-n}{n^3}\frac{1}{gD_{n50}}$ and (2.9)

$$c = \frac{1 + \gamma \frac{1-n}{n}}{ng} \tag{2.10}$$

The expressions for the coefficients a [s/m], b [s^2/m^2] and c [-] have derived theoretically, while the dimensionless coefficients α and β have to be determined experimentally. Coefficients a, b and c depend mainly on the Reynolds number, the stone shape and grading, while α and β depend on the grading and the shape of the stones. Without any further information, α=1000 and β=1.1 can be used as a good first estimation. Here it should be noted that the last term in equation (2.7) can be ignored for scaling porous flow [Burcharth et al, 1999].

The celerity of the waves is given by the following formula

$$\upsilon = \frac{L}{T} \tag{2.11}$$

Porous flow is the expression used for flow through a granular medium, like sand, pebbles or stones. The loads due to porous flow often come from the soil side of the interface soil-water. Porous flow can be either turbulent or laminar, but for coarse material the flow is usually turbulent. Coarse materials are used in filters, sills, breakwaters.

With this equation the flow in a porous medium can be calculated.

$$v_f = n * v \tag{2.12}$$

Pore velocity is affected by the porosity of the mean. Turbulence can play an important role in pressures and velocities as well, especially for breakwater with submergence factor greater than zero.

Linear wave theory indicates different formulas for particle velocity considering the relative depth. Of course these formulas apply only before and after the breakwater and in no case inside it.

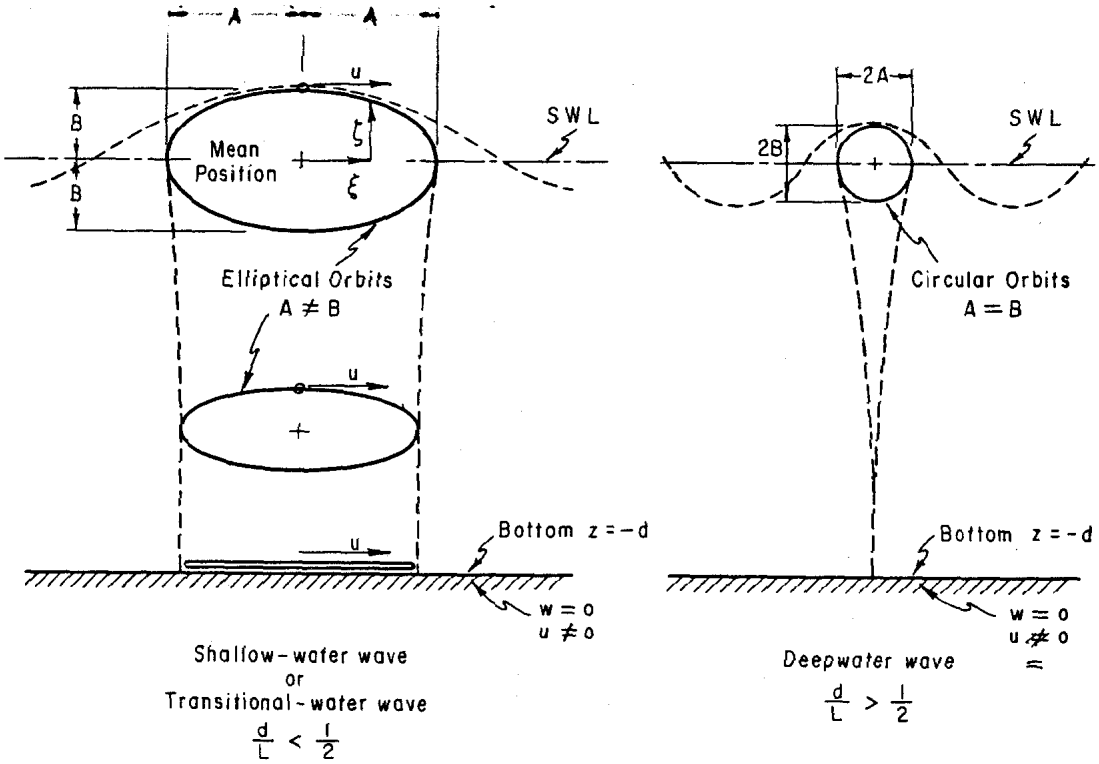

Figure 2.3 Linear wave theory figures

Linear wave theory

Relative depth Characteristics	Shallow water $\frac{d}{L}<\frac{1}{20}$	Transitional water depth $\frac{1}{20}\le\frac{d}{L}\le\frac{1}{2}$	Deep water $\frac{d}{L}<\frac{1}{2}$
Particle velocity			
Horizontal	$u = A\sqrt{\frac{g}{d}}\sin\theta$	$u = \omega A\frac{\cosh K(d+z)}{\sinh Kd}\sin\theta$	$u = \omega A e^{Kz}sin\theta$
Vertical	$w = \omega A\left(1+\frac{z}{d}\right)\cos\theta$	$w = \omega A\frac{\sinh K(d+z)}{\sinh Kd}\cos\theta$	$w = \omega A e^{Kz}sin\theta$

Table 2.1 Linear wave theory formulas

$$A=\frac{h}{2} \qquad \omega=\frac{2\pi}{T} \qquad K=\frac{2\pi}{L} \qquad \theta=\omega t-kx$$

Pressure gradients inside breakwater

In a homogeneous porous media exposed to harmonic waves the amplitude of pressure oscillation will decrease exponentially in the direction of wave propagation according to the following expression [Biesel 1950, Le Mehaute 1957, Oumeraci 1990, et al]:

$$p_{\max}(x) = \rho_w g \frac{h}{2} e^{-\delta \frac{2\pi}{L'} x} \tag{2.13}$$

where x=0 corresponds to the surface between armour layer and core.

According to Burcharth [1999] it seems that there is a linear relationship between pressure and wave height for constant period as well as pressure and period for constant wave height. The relation between velocity and pressure gradient is written as follows:

$$v_f = k i^{\frac{1}{p}} \tag{2.14}$$

in which k is the permeability [m/s] of the porous material. For laminar flow, p=1, the Forchheimer equation reduces to Darcy's law and k is the inverse of α in equation (2.7). For turbulent flow, p=2.

It is also interesting to see how the pressure gradient varies across the breakwater and especially between the front and the back face of it. It is chosen to study this at the half height of the breakwater and starting under the first line of stones. The reason behind that is that the half height of the breakwater is considered to be characteristic height for the flow inside it and also it would be interesting to study the intermediate point between the changes of the two means.

It is important to study if it would be a constant gradient across it or if it would be a difference between front face gradient and back face one. If not it is also interesting to see what would the parameters be affecting the angle of the line.

Linear wave theory

Relative depth Characteristics	Shallow water $\frac{d}{L} < \frac{1}{20}$	Transitional water depth $\frac{1}{20} \le \frac{d}{L} \le \frac{1}{2}$	Deep water $\frac{d}{L} < \frac{1}{2}$
Subsurface pressure	$p = -\rho g z + \rho g A \sin\theta$	$p = -\rho g z + \rho g A \frac{\cosh K(d+z)}{\cosh Kd}$	$p = -\rho g z + \rho g e^{Kz} A \sin\theta$

Table 2.2 Linear wave theory formulas

$$A = \frac{h}{2} \qquad \omega = \frac{2\pi}{T} \qquad K = \frac{2\pi}{L} \qquad \theta = \omega t - kx$$

As linear wave theory indicates, there is not much influence of wave height to the subsurface pressure. Also here formulas can be applied only before and after the breakwater and not inside it.

The Forchheimer equation for turbulent flow as well as the Darcy law can help us bond velocities and pressure gradients together and see in which way they are connected together.

From Bernoulli:

$$h_i = z_i + \frac{P_i}{\gamma_w}, \text{ where } \gamma_w = \rho_w * g$$

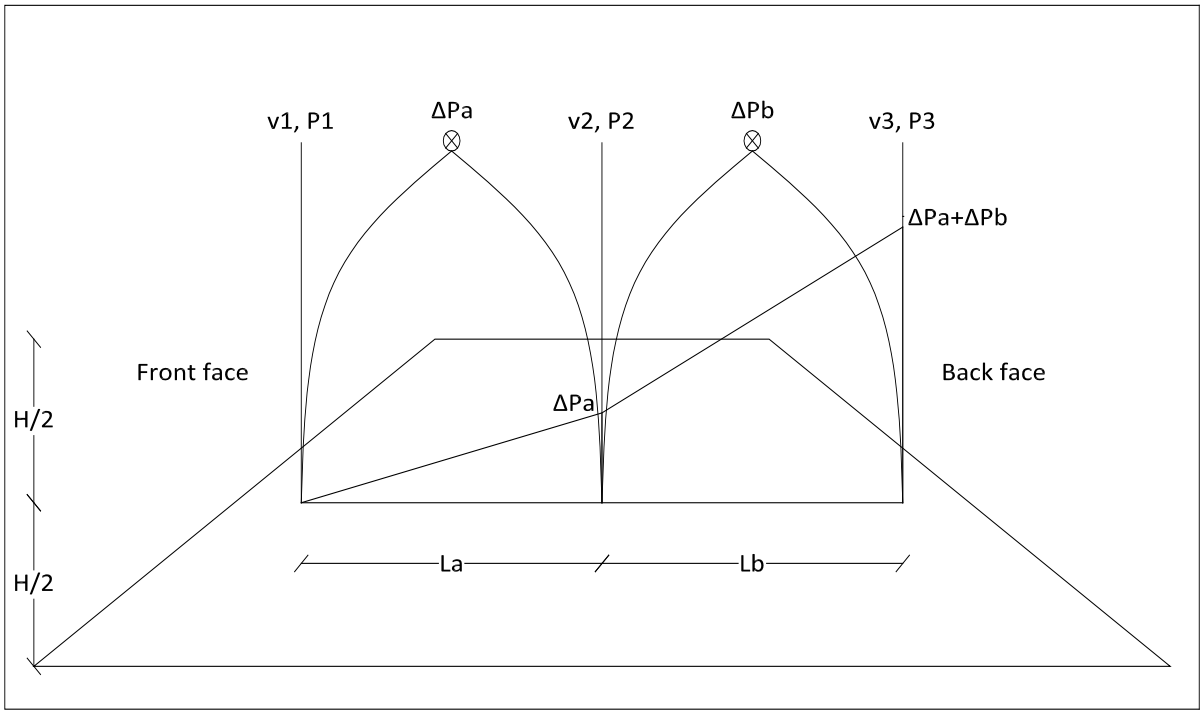

Figure 2.4 Pressure gradients along the breakwater

For points 1,2 and 3 we have:

$$h_1 = z_1 + \frac{P_1}{\gamma_w}$$

$$h_2 = z_2 + \frac{P_2}{\gamma_w}$$

$$h_3 = z_3 + \frac{P_3}{\gamma_w}$$

For the study of the hydraulic pressure is at the front and back face the structure the following procedure was made.
For the front face it is:

$$\Delta h_{12} = h_2 - h_1 = (z_2 - z_1) + \frac{P_2 - P_1}{\gamma_w} = 0 + \frac{\Delta P_a}{\gamma_w} = \frac{\Delta P_a}{\gamma_w}$$

And for the back face it is:

$$\Delta h_{23} = h_3 - h_2 = (z_3 - z_2) + \frac{P_3 - P_2}{\gamma_w} = 0 + \frac{\Delta P_b}{\gamma_w} = \frac{\Delta P_b}{\gamma_w}$$

Burcharth [1999] equation for turbulent flow (p=2) is:

$v_f = k * i^{1/2}$ and $i = \frac{\Delta h}{L}$, where L is the distance between the points.

So for points 1 and 2: $v_f{}^{12} = k * i^{1/2} = k * \left(\frac{\Delta h_{12}}{L_a} \right)^{1/2} = k * \left(\frac{\Delta Pa}{\gamma_w * L_a} \right)^{1/2}$

But also, $\upsilon_f = n * \upsilon$

So, finally we have:

$$\boxed{v_{12} = \frac{k}{n} * \left(\frac{\Delta P_a}{\gamma_w * L_a} \right)^{1/2} = f(\Delta P_a{}^{1/2})} \quad (2.15)$$

Following the same path for points 2 and 3 of the back face of the structure the following formula has derived:

$$\boxed{v_{23} = \frac{k}{n} * \left(\frac{\Delta P_b}{\gamma_w * L_b} \right)^{1/2} = f(\Delta P_b{}^{1/2})} \quad (2.16)$$

This lead to the conclusion that flow velocity inside the breakwater is a function of the pressure gradient. But of course this also means that pressure gradient is a function of the flow velocity inside the structure.

So formulas (2.14) and (2.15) can be:

$$\boxed{\Delta P_a = \left(\frac{v_{12} * n}{k} \right)^2 * \gamma_w * L_a} \quad (2.17)$$

and

$$\boxed{\Delta P_b = \left(\frac{v_{23} * n}{k} \right)^2 * \gamma_w * L_b} \quad (2.18)$$

In this case: $v_{12} = v_2 - v_1$ and $v_{23} = v_3 - v_2$

2.6. Conclusions

The main conclusions that can be drawn from the above literature presentation are the following:

2.6.1. Velocities inside the breakwater

Although there is some theoretical background, not much research has been conducted which identifies the velocities inside a homogeneous submerged breakwater. Porosity, average and local, plays an important role of the velocities that occur inside the structure. From an environmental point of view, it needs to be studied the real velocity but also the flow velocity to say if a breakwater can sustain marine life.

2.6.2. Pressure gradients inside the breakwater

It is clear that pressure gradients are closely connected to water flow and thus velocities inside a breakwater. Since velocities are quite difficult to measure, pressure gradients can distribute in order to draw safe conclusions about the water move inside the breakwater.

3 LABORATORY RESEARCH

This chapter describes the experimental study of this research. First, the required prototype for the breakwater and the final dimensions are defined. The scaling process is based on this prototype and leads to the scale model. Lastly, the laboratory equipment, experiment set and experiment set-up are discussed and the initial test plan is presented.

3.1. Prototype

The first main issue in the set-up process of a physical model is the assumption of a proper prototype. The prototype should be a rather simple structure, yet representative for a large range of cases. With the help of scale effects and similarity requirements this prototype will form the basis for the design of the scale model.

The prototype consists of a simplified homogenous rock structure, which means that some relevant dimensions and conditions are excluded. Also, the hydraulic conditions ignore the existence of oblique waves and wind effects.

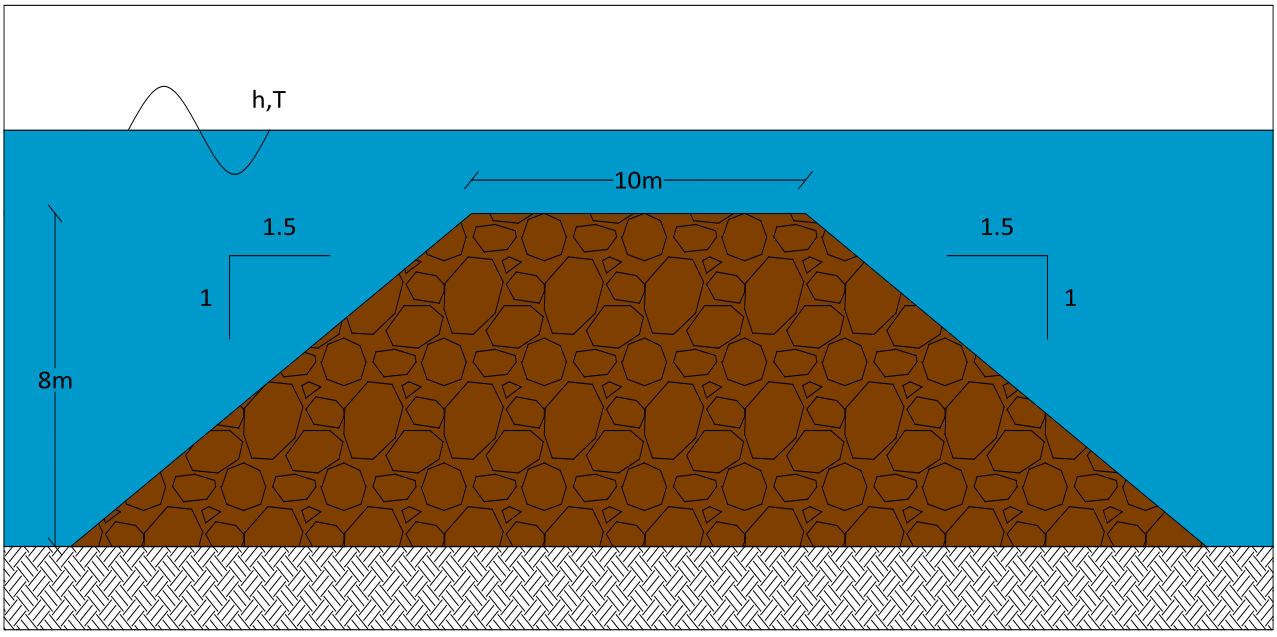

Figure 3.1 Cross section of prototype breakwater

3.1.1. Dimensions and hydraulic conditions

In order to create a representative scale model, it is necessary to assume a prototype of a submerged breakwater. With the help of scale effects and similarity requirements this prototype will form the basis for the design of the scale model.

For this research, the prototype consists of a simplified rock protection structure. Several aspects have been excluded like a berm and a toe structure. The influence of the wind and the existence of oblique waves are not taken into account due to lack of proper simulation equipment.

The dimensions of this typical coastal structure as shown in Figure 3.1 are:

Total height: 8m

Crest width: 10m

Slope: 1.5: 1 (H: V)

Water depth: d= 8m

Wave height: h= 0.5*d= 4m

Wave steepness: s= 0.03-0.06

A rule of thumb for these hydraulic conditions is:

Waves break for:

- s>1/7 or h>0.15L

- h>0.75H

So, it must be ensured that waves won't break before they reach the breakwater.

3.1.2. Breakwater stability

The stability of submerged structures is usually higher than for non-overtopped structures, due to the fact that the wave energy can pass over the crest, leading to lower wave forces on the armor layer of the seaward slope. Usually for submerged structures, the stability at the water level close to the crest level will be most critical. Stability is only a function of the relative crest height H_c/H, the damage level S and the spectral stability number Ns. The stability in terms of a final stable crest height (H_c') is described by [Pilarczyk and Zeidler, 1996] and [Pilarczyk, 2003]:

$$\frac{H_c'}{H_c} = (2.1 + 0.1S)e^{-0.14N_s^*} \tag{3.1}$$

This formula can be applied for regular waves as well as random ones. The natural limiting values of the relative crest height H_c'/H are 1.0 (no damage at all) and 0.0 (no breakwater) respectively. The three levels of damage are: (a) S=2, start of damage, (b) S=5-8, moderate damage and (c) S=12 severe damage (more than one layer removed from the crest). The spectral stability number N_s^* is given by the following formula:

$$N_s^* = \frac{h_s}{\Delta D_{n50}} s^{-\frac{1}{3}} \tag{3.2}$$

For a chosen crest height (H_c), accepted damage level (S) and given water level (h), wave height (H) and period (T), the required D_{n50} can be calculated and the required stone weight (W_{50}) can be determined.

A first estimation of the Dn_{50} is given below:

$$\frac{H_c'}{H_c} = (2.1 + 0.1S)e^{-0.14Ns^*} \Rightarrow 1 = (2.1 + 0.1*0)e^{-0.14Ns^*} \Rightarrow N_s^* = 5.3$$

$$Ns^* = \frac{h_s}{\Delta D_{n50}} s^{-\frac{1}{3}} \Rightarrow 5.3 = \frac{4}{1.7 * D_{n50}} 0.03^{-\frac{1}{3}} \Rightarrow D_{n50} = 1.46m$$

3.1.3. Material

The breakwater is a rubble-mound type, so it is constructed with quarry stones. Also, it is a homogenous breakwater, so there are no layers, underlayers or filters, just completely constructed by stones that would usually be used for the armour layer of a conventional breakwater. The reason why it was decided not to use core for the breakwater is because we are interested in high and constant porosity across the breakwater so that it can maintain marine life.

Rock material: stone class 6-10tons

D_{n50}= 1.46m

D_{15}=1.50m D_{50}= 1.70m D_{85}= 1.95m

Shape parameter= 0.84

Grading: narrow grading D_{85}/D_{15}= 1.3

Narrow grading was chosen due to the absence of core layer. It was assumed that this homogenous rubble-mound breakwater was built totally out of armour layer stones.

3.2. Scaling process

3.2.1. Froude criterion

A parameter that expresses the relative influence of inertial and gravity forces in a hydraulic flow is given by the square root of the ratio of inertial to gravity forces. The Froude criterion for modeling flows can be described as

$$\frac{N_V}{\sqrt{N_g N_L}} = 1$$

This criterion is valid for flows of which the inertial forces are balanced primarily by the gravitational forces, which is the case in most flows with a free surface. Consequently, the Froude model law is the most important criterion to be considered when designing a coastal scale model.

3.2.2. Reynolds criterion

When viscous forces dominate a hydraulic flow, the important parameter is the ratio of inertial to viscous forces given by the Reynolds number. The Reynolds criterion for modelling flows can be described:

$$N_V N_L = 1$$

This criterion is important when viscous forces dominate the hydraulic flow. Obviously, the Reynolds criterion does not correspond to the Froude criterion. This means that gravity and viscous forces cannot be processed in the same scale model. If gravity is important, viscous forces have to be reduced to a minimum.

3.2.3. Geometric similarity

Geometrical similar models are also known as geometrical undistorted models. Geometrically undistorted models are models in which the vertical and horizontal scales are the same, and they represent the true geometric reproduction of the prototype.

3.3. Scale model

The similarity criteria result in the final dimensions and material properties of the scale model.

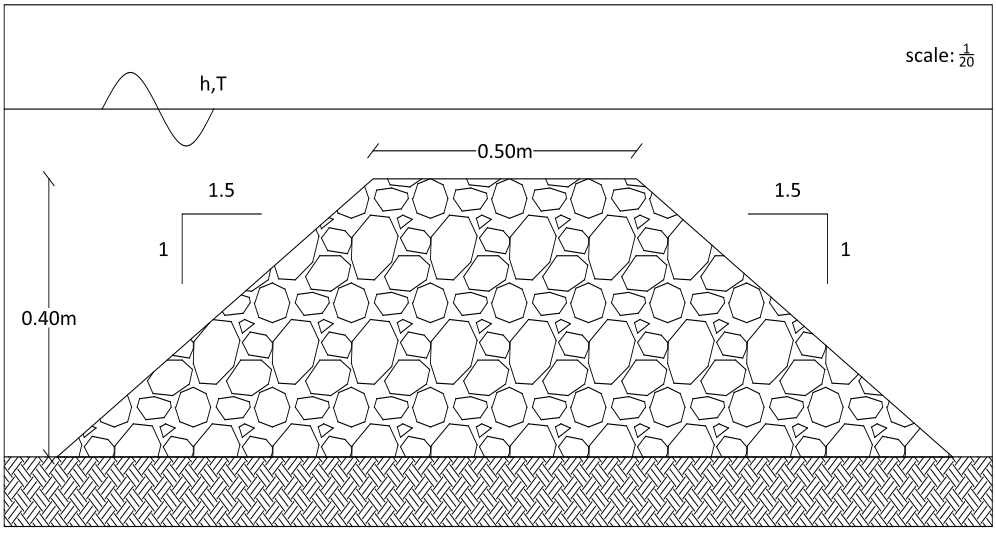

Figure 3.2 Scale model

3.3.1. Dimensions and hydraulic conditions

As shown in Figure 3.2 the dimensions of the scale model are:

Scale: 1/20

Total height: 0.40m

Crest width: 0.50m

Slope: 1.5: 1 (H: V)

Water depth: h= 0.40m

Wave height: H= 0.5*h= 0.20m

Wave steepness: s= 0.031

The permeability of the stones was found k=0.1m/sec.

3.3.2. Scale model stability

Same as with the prototype the (3.1) and (3.2) formula is used to define the stability of the breakwater in scale model.

$$\frac{h_c'}{h_c} = (2.1 + 0.1S)e^{-0.14Ns*} \Rightarrow 1 = (2.1 + 0.1*0)e^{-0.14Ns*} \Rightarrow N_s^* = 5.3$$

$$Ns* = \frac{H_s}{\Delta D_{n50}} s^{-1/3} \Rightarrow 5.3 = \frac{0.2}{1.7 * D_{n50}} 0.03^{-1/3} \Rightarrow D_{n50} = 0.073m$$

3.3.3. Material

The hydraulic similitude results in the following material properties of the scale model:

D_{n50}= 73mm

D_{15}= 75mm D_{50}= 85mm D_{85}= 97.5mm

M_{15}=1.11kg M_{50}= 1.62kg M_{85}= 2.45kg

Shape parameter= 0.84

Grading: narrow grading D_{85}/D_{15}= 1.3

Since there was no material with such grading, a manual selection from material with very large grading was made.

The size of the pores was considered large compared to the size of the laboratory equipment used.

It is also very important to mention here that the breakwater was constructed in a way that the average pore of the structure was almost the same. Great attention was given when the laboratory equipment was placed inside the breakwater so that the local porosity did not deviate much. Yet, the size of the pores was picked accidentally and it could not be accurately defined or measured so there might be a difference to the results due to this fact. This sentence will be discussed further later on.

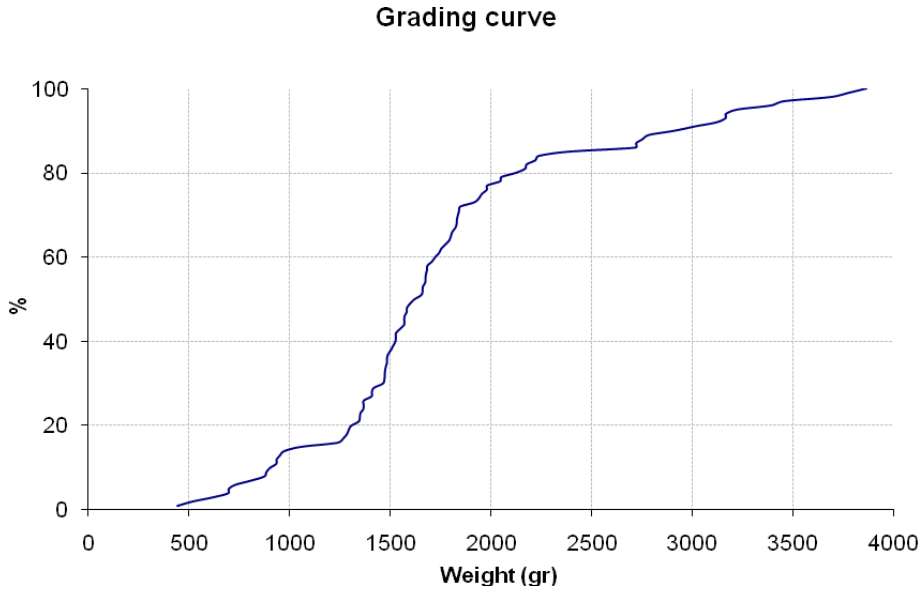

Figure 3.3 Grading curve of the material used

The specific density of this material was found ρ=2625 kg/m^3.

3.4. Laboratory equipment

3.4.1. Hydraulic equipment

3.4.1.1. Wave flume

This experimental research was performed at the wave flume "Lange Speurwerk Goot" at the Fluid Mechanics Laboratory of TU Delft. The characteristics of this flume are:

- Length= 40m
- Width= 0.80m
- Height= 0.80m

The walls consist of glass allowing a full observation of the process. The flume can be filled and emptied with pump valves on both sides.

Picture 3.1 Wave flume at Fluid Mechanics Laboratory of TU Delft

3.4.1.2. Wave generator

The wave flume is equipped with a wave generator. This wave generator has Active Reflection Compensation (ARC) and a second order wave generation technique, which means that the second-order effects of the first higher and first lower harmonics of the wave field are taken into account in the wave generator motion.

The wave generator is controlled with the use of DASYLab, software developed by National Instruments. The function of the generator is determined by a steering file which contains all the wave information: the requested wave height and period, the type of the spectrum (JONSWAP, Pierson/Moscowitz, simple sinusoidal etc.), its characteristics (peak-enhancement factor, peak width factor) and the duration. This steering file is created with the help of software developed by Deltares and basically consists of an electrical wave records which controls the movement of the pedal.

The user needs to create a steering file in which various parameters are defined: the water depth in the flume, the required wave height and the required wave length for regular waves. The peak-enhancement factor, peak-width factor and duration of the spectrum (last 3 parameters only for JONSWAP-spectra) have to be identified when random wave tests take place. This steering file is created with the help of software developed by *Deltares* and basically consists of an electrical wave record which controls the movement of the pedal.

3.4.2. Measuring equipment

3.4.2.1. Wave gauges

Two sets of three wave gauges are installed inside the wave flume. The first set is placed just in front of the breakwater and the other set is placed behind the breakwater. The differences in voltage between the two poles of the wave gauge are converted in the differences in water level. The water levels and corresponding voltages are established by several calibrations of the wave gauges. This calibration is executed by measuring the voltage for several known water levels.

The set of three wave gauges is necessary to calculate the wave height and wave period of the waves traveling to the structure. The wave gauges measure the differences in water level, but this is the interaction between incoming and reflected waves. Because the three wave gauges in a set are installed at a certain known distance from each other, a Matlab-code can distinguish the incoming and reflected wave. This results in the relevant incoming significant wave height (H) and wave period (T).

Picture 3.2 Flume close-up

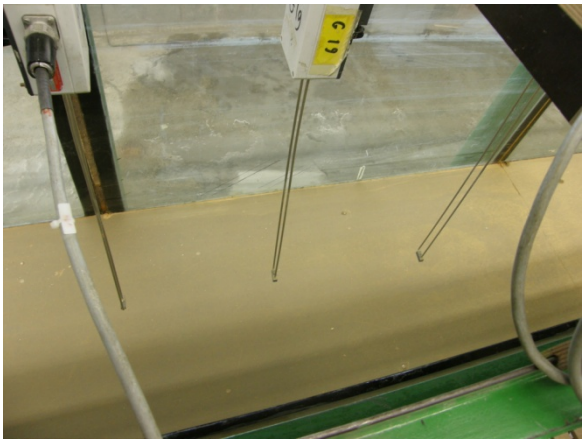

Picture 3.3 Wave gauges

3.4.2.2. Pressure sensors

Pressure difference inside the breakwater is measured with the help of pressure transducers. They are miniature pressure sensors providing reliable differential pressure sensing performance. Their accuracy is close to 1% and range ±3.4kPa, which is a lot larger than the range required.

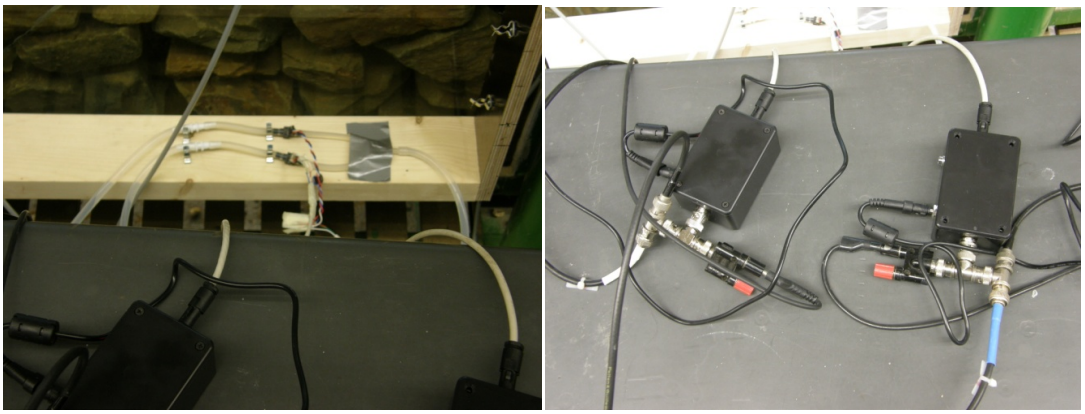

Picture 3.4 Pressure sensors

3.4.2.3. Velocity transducers

In order to measure velocity inside a porous media such as a breakwater, electromagnetic flow meters were used. The accuracy is 1% while the range varies from -100cm/sec to +100cm/sec.

The velocity transducers were used in this study to measure the local maximum velocity inside the pores of the structure. From the signal occurred in every test the RMS velocity was extracted each time.

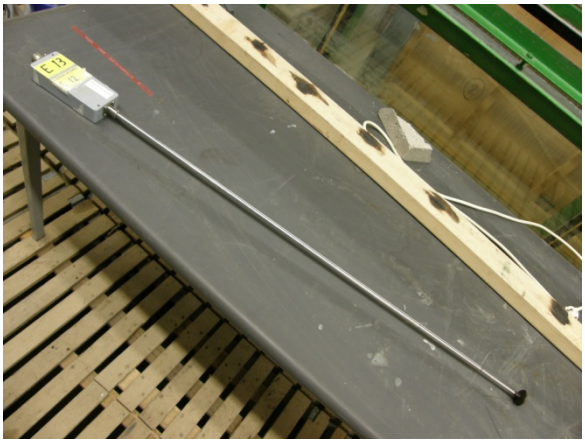

Picture 3.5 Velocity transducer

3.5. Experiment setup

3.5.1. Varying parameters

3.5.1.1. Wave height

Varying the wave height was not very difficult; it could be done by changing the wave height settings in the steering file for the wave generator.

Because of the ARC, the wave generator was only able to create waves up to a certain maximum wave height. For that reason, the significant wave height (H_s) in this research varied between 0.01m and 0.10m for regular waves.

3.5.1.2. Wave steepness

Wave steepness is an alternative parameter of wave period. Again, the range was limited by wave generator (limited pedal movement).The range of the wave steepness used is 3-6%

3.5.1.3. Water depth

It is very interesting to see how the output data (pressure and velocity) will vary for same waves (H, s) but with different water depths. This factor is quite important for submerged structures and it is known that water depth varies according to tidal conditions.

3.5.2. Experiment code

Experiment codes are used to clarify the large amount of various experiments.

The experiment code is a combination of the relevant parameters in the experiment:

· Type of experiment

· Wave height [m]

· Wave steepness [-]

· Water depth [m]

· Velocity [m/sec]

· Pressure gradient [Pa]

3.6. Test program

It has chosen relatively low wave heights, indeed a lot lower than design wave conditions. The main reason to do that is to see if there is adequate water renewal inside the breakwater even during summertime when wave heights that occur are small.

The same set of experiments has repeated for three different water depths (or submergence factors) to see how the water depth can influence water circulation (and thus water renewal) inside a porous media such as homogenous rubble-mound breakwater.

3.7. Final measurement set-up

The final measurement system with scale model is shown in the Figure 3.6.

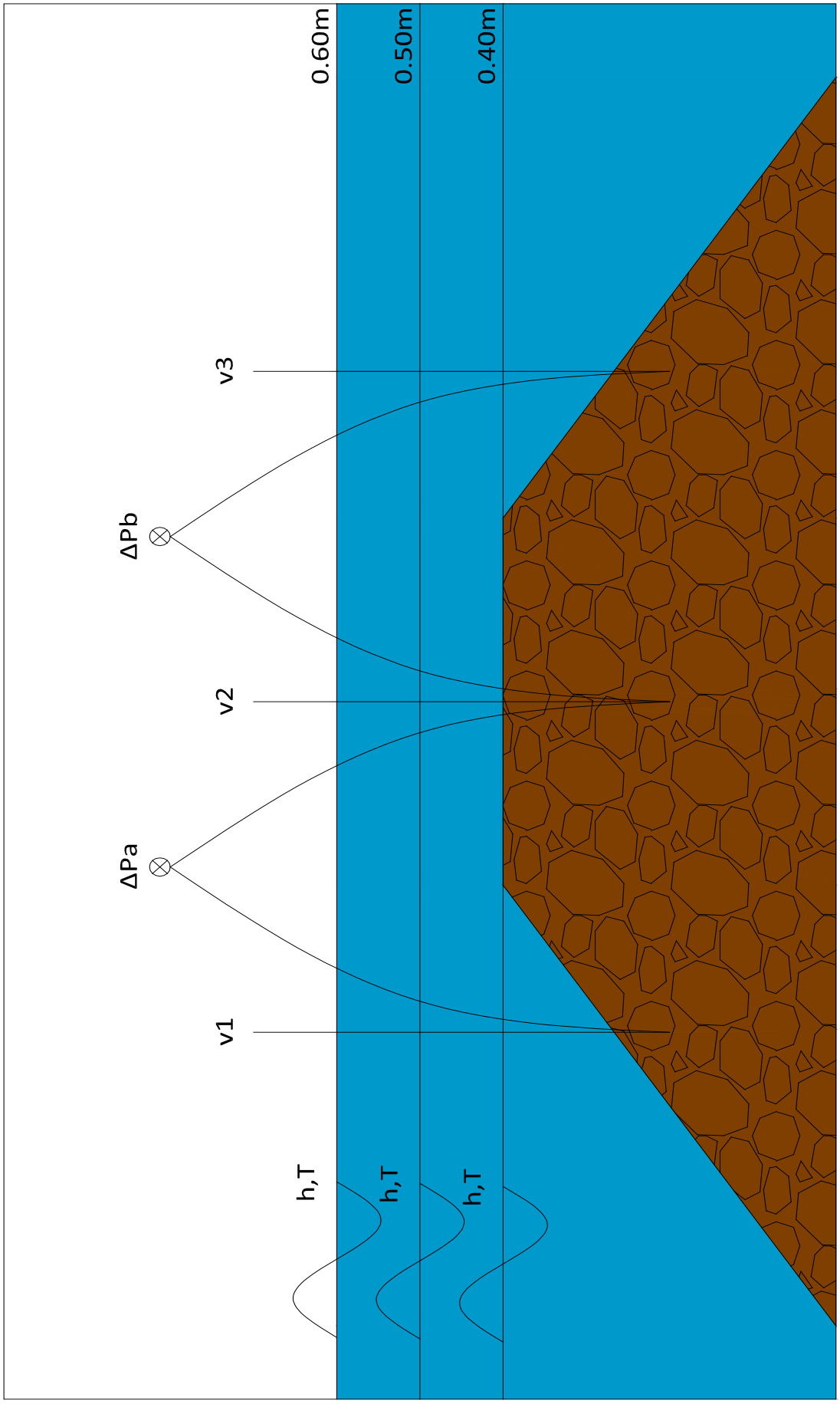

Picture 3.6 Experimental set-up

4 ANALYSIS OF EXPERIMENTAL RESULTS

4.1. Introduction

In this chapter the results derived from the experimental work are being presented. The analysis of the experimental results is divided in two main sections: velocities and pressure gradients. The behaviour of the varied breakwater parameters will be discussed and compared with the elements of the literature study of Chapter 2.

Furthermore, it should be mentioned that the size of the voids where the velocity and pressure meters where placed, were selected randomly. This fact plays an important role to the results occurred as it is clear that it is almost impossible that the voids have the exact same size. The size of the voids occurred in the scale model is mainly depending on the way the stones were put together. For more accurate results, this procedure should have been performed multiple times to safely determine an average void size.

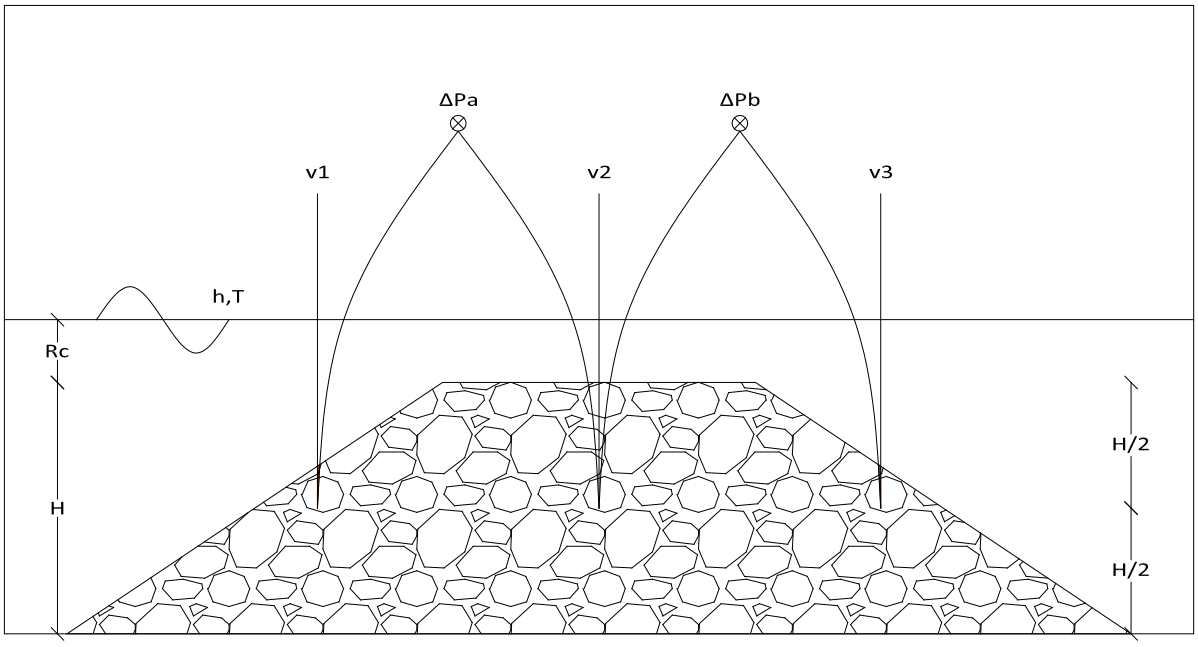

Figure 4.1 Cross section of breakwater

4.2. Water velocity inside breakwater

4.2.1. Wave height and stone diameter

One of breakwaters' primary functions is to change and control the wave climate. This happens due to changes in wave celerity when waves meet the breakwater. Especially for rubble-mound submerged breakwaters. It is interesting to see how the wave height influences the velocities inside such a breakwater, what the changes of the other parameters are and how they vary across the breakwater.

First of all, the influence of the wave height on the pore velocity has to be elaborated as well as the effect of the stone diameter chosen. It is clear that larger velocities occur for smaller D_{n50}/h ratios because then, there are larger wave heights for constant nominal diameter. When the D_{n50} decreases for constant wave heights, then velocities decreases as well due to the reduction of the porosity of the breakwater.

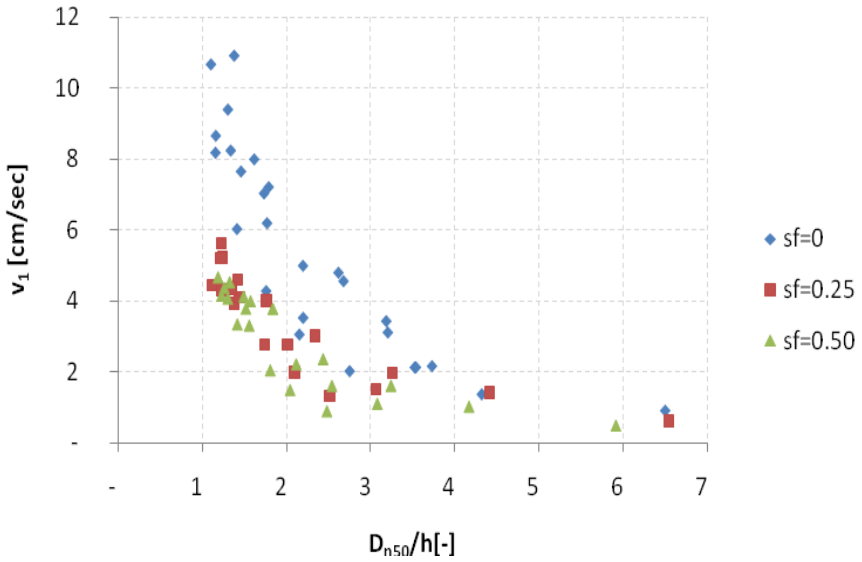

Figure 4.1.1 D_{n50}/h over RMS measured velocity v_1 for different submergence factors

From Figure 4.1.1, it can be noticed that the velocity measured at the front face of the breakwater has different ranges for different submergence factors. The influence of the wave height (or stone diameter) is much larger when submergence factor is zero. The influence of the D_{n50}/h ratio on the velocity becomes lower for bigger submergence factors because of the turbulence inside the breakwater and thus the energy loss, especially for submergence factors larger than zero. Furthermore, submergence factor is important to wave breaking at the front part of the breakwater, which occurs for submergence factors near zero.

When the crest of the breakwater and water level are equal, then the only way for water to get through the breakwater is via the pores. When submergence is greater than zero water can pass through the pores of the breakwater or over the structure (the R_c zone). So, for

fully submerged breakwaters there is more water circulation in the R_c zone than inside the breakwater of course because of the larger permeability of the water over the stone.

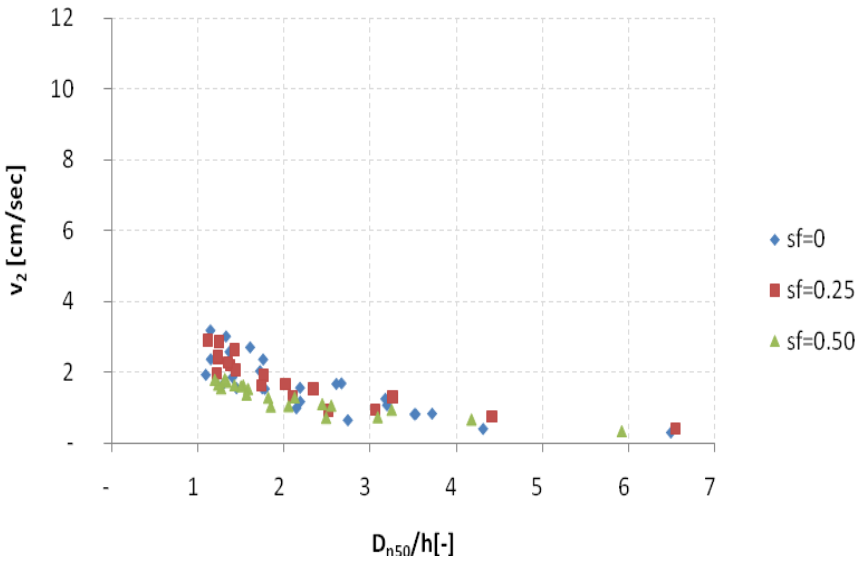

Figure 4.1.2 D_{n50}/h over RMS measured velocity v_2 for different submergence factors

Moving from the front slope of the breakwater to the middle of it, there are many things that change. The velocity in the middle of the breakwater is the smallest compared with the ones on the front and back of it, as is elaborated later. The main reason why the velocities are smaller in the middle of the breakwater is the loss of energy occurred mainly in the front face but also the difference in the size of the voids. Also, the influence of the D_{n50}/h parameter is distinctively lower. In the middle of the breakwater the height of the structure is constant while at the front and back face it is not constant, which leads to distinctively smaller turbulence and more stable flow in these areas and thus smaller velocities.

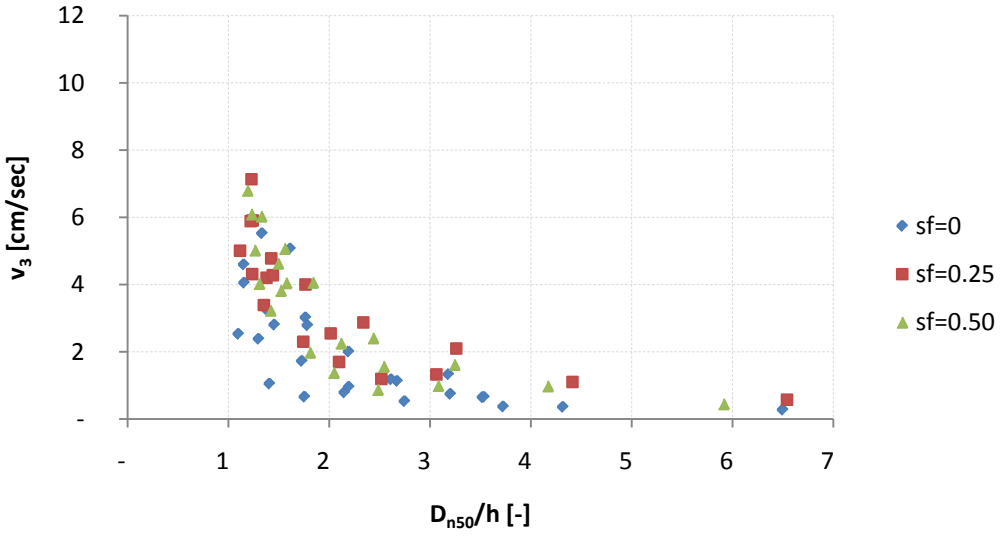

Figure 4.1.3 D_{n50}/h over RMS measured velocity v_3 for different submergence factors

Velocities at the back of the breakwater (Figure 4.1.3) are closely related to the ones in the front, mainly because of turbulence on the slopes of the breakwater as the cross-section is changing continuously, as well as the symmetry of the breakwater and the flume. This means that the velocities at the front and at the back have similarities compared to the velocity in the middle, which it can be said it's in a different category. The main difference here is that submergence does not play a very important role as in velocity v_1. This has basically to do with the breaking of waves in the front of breakwater and the reflection and transmission occurs at the back of the structure.

It is also very important to mention that although the section for the breakwater is symmetrical, the flow of the water inside it is not so it is expected to see some differences occurring between the front and the back face of it. Submergence does not affect the velocity at the back face, mainly because of the breaking of the waves at the front face as well as energy dissipation due to wave breaking that lead to smaller values of velocity there. Lastly, velocities at the back face of the structure are as large as the ones at the front. A possible explanation is that this is caused by the reflection of the waves at the wave board.

4.2.2. Submergence factor

4.2.2.1. Water acceleration

Without doubt, submergence is one of the most important characteristics of a submerged breakwater. It is clear that submergence is also connected to transmission. The following figures show a direct relation between horizontal particle velocity before the breakwater at the same height as the velocity meters were placed. It is to be mentioned here that the maximum local velocity was measured and not the filter velocity. The purpose of the graphs is to show a qualitative approach about how velocities can vary depending on the water motion before a breakwater.

But also it has to be mentioned that not only velocity is a function of wave height, but also velocity difference (acceleration):

$$v_i - v_j = f(h_i) - f(h_j) = \kappa(h_i - h_j) = \kappa(h_i - C_t h_i) = \kappa(1 - C_t)h_i = f(h_i) \quad (4.1)$$

Velocity at the front part of the breakwater makes a large difference for zero submergence, compared to other velocities or submergence factors. Actually, for zero submergence the velocities at the back of the structure (velocity difference between v_2 and v_3) are much lower, which validates the statement that waves break at the front part of breakwater when submergence is zero. So, a large part of the energy is lost at the front part of the breakwater and transforms into water velocity. Also, for submergence other than zero, velocity differences are quite low and they don't differ between them.

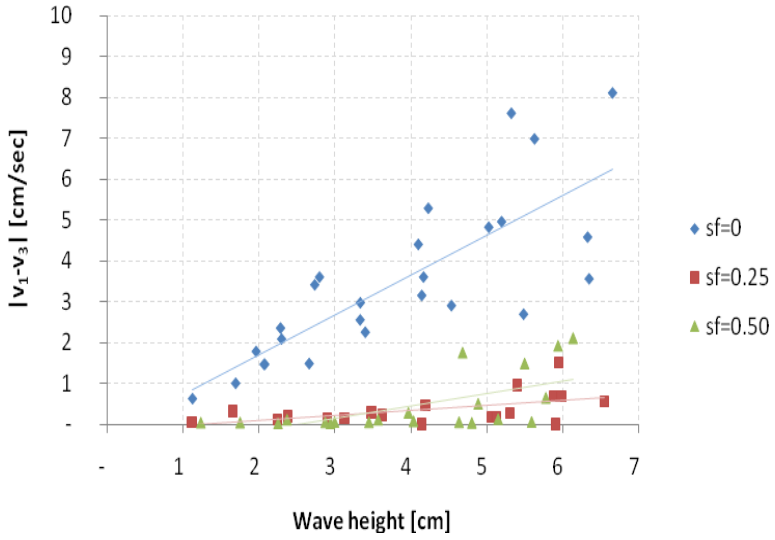

(a)

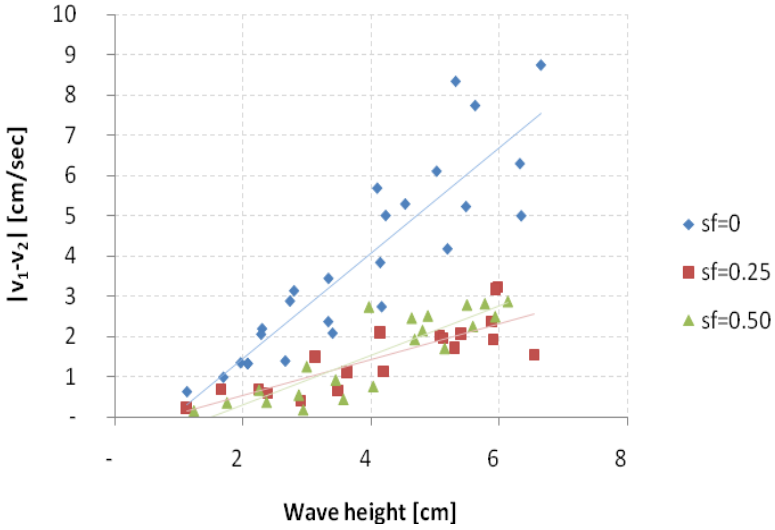

(b)

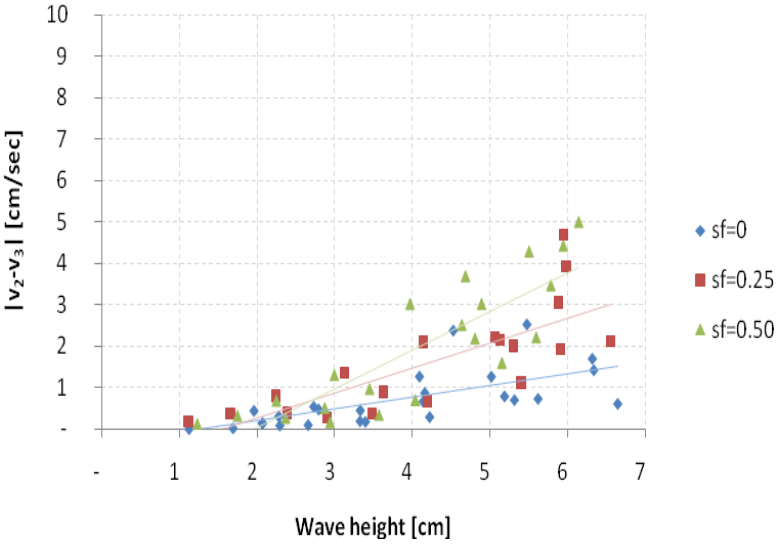

(c)

Figure 4.2 Wave heights over velocity differences for different submergence factors.

Figure 4.2(a) shows the large values of velocity in front of the breakwater compared with the velocity in the middle and at the back for zero submergence. This difference is caused by the breaking of the waves in the front of the breakwater. Furthermore, zero submergence plays an important role in this procedure as waves interact directly with the structure.

As shown in Figure 4.2(b) acceleration at the front part of the breakwater is a lot larger for zero submergence compared to submergence factors greater than zero, once again because of the breaking of waves upstream and the turbulence has a consequence on it. It could be assumed that when it comes to water acceleration, zero submergence falls into a different category than submergence factors larger than zero.

In Figure 4.2(c) it can be seen how velocity differences at the back part of the breakwater vary in relation to the incoming wave height. Here, submergence has an inverse influence; the higher the submergence factor the larger velocity difference occurs with the same wave height. This makes sense only if it is considered that the lower the submergence is the more energy loss there is due to wave breaking and thus less energy is transferred to the second part of the breakwater.

Furthermore, it is very interesting to see that velocity in the middle of breakwater is the lowest in all different cases. Probably, this has to do with the size of the voids that the velocity meters are placed in as well as the turbulence that is less intense in that part of the breakwater.

4.2.2.2. Wave period

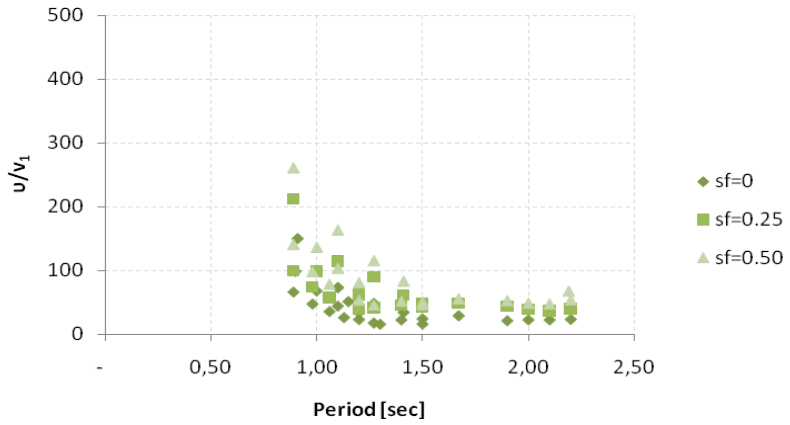

Figure 4.3.1 Relation between T and u/v_1 for different s.f.

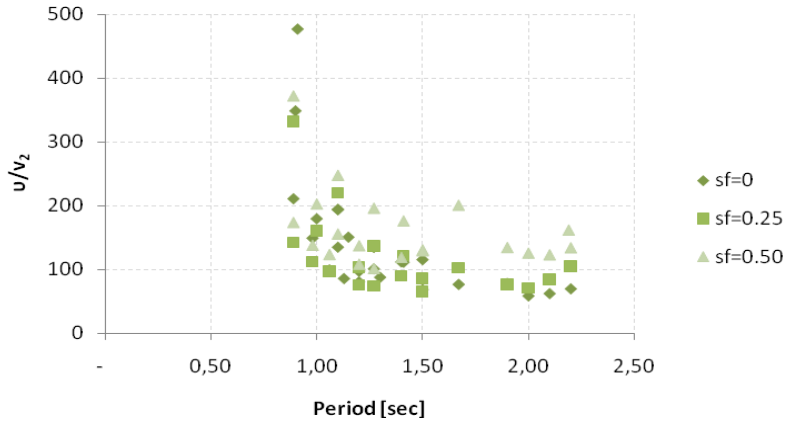

Figure 4.3.2 Relation between T and u/v_2 for different s.f.

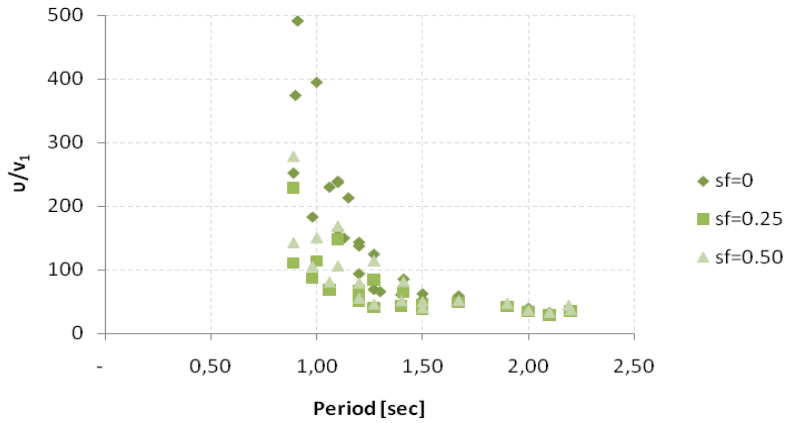

Figure 4.3.3 Relation between T and u/v_3 for different s.f.

Of course, wave period and thus wave steepness influences the character of the waves and the velocities occurred for different submergences. Considering Figure 4.3.1 it can be seen that the dissipation is very low as the trends have a fixed distance between them. The physical reasoning for the distance between the lines is because of the different water levels (submergence). Figure 4.3.3 shows that for smaller waves the ratio u/v_3 is larger for smaller periods which mean that the velocity v_3 decreases also for short waves. This is because smaller waves have smaller resistance, energy and mass and thus lower velocities occur compared to waves with the same wave height but longer period. Also, in this figure the gradient of the sf=0 trend is a lot steeper than the other trends of the same graph as well as for Figures 4.3.1 and 4.3.2.

The reason behind this phenomenon is that as the wave is breaking at the front of the breakwater the flow of the water is given a horizontal direction again after the breaking which of course affects the measured velocity at that place. As for Figure 4.3.2 it cannot be drawn a safe conclusion. Possibly this is the transitional step between Figures 4.3.1 and 4.3.3.

4.2.2.3. Particle velocity upstream

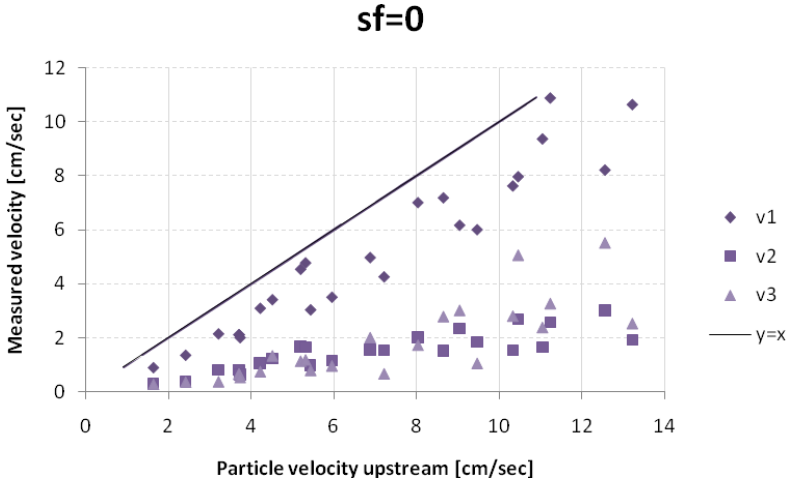

Figure 4.4.1 Calculated velocities as a function of RMS measured for s.f. =0

Figure 4.4.1 shows that for zero submergence the velocity in front of the breakwater is much lower than in the front face of it, while in the middle and in the back of the breakwater the difference is not that much. Here as well, velocity v_2 is the lowest compared to the other two as it was seen in the Figures 4.1.2 and 4.3.2.

What is interesting to see is that velocities at the front face of the structure are generally larger than the particle velocity upstream, while v_2 happens to be smaller than the particle velocity in front of the breakwater. This phenomenon is connected with the change of the medium and so the permeability at the front and back of the structure. When water meets or leaves the breakwater, in that area larger velocities occur as a result of the medium change.

For submergence 0.25 and 0.50 it can be seen that the following graphs have main similarities. In both Figures 4.4.2 and 4.4.3 it is clear that the velocities in the front and back slope are bigger than the velocities in front of the breakwater at the same height as the velocities were measured. Also, velocities in the middle of the breakwater seem to have no difference to the water velocity before the breakwater. Here as well, considering the similarities of the Figures 4.4.2 and 4.4.3, it feels that zero submergence is a different situation compared to submergence larger than zero.

O f course in all Figures 4.4.1, 4.4.2 and 4.4.3 particle velocities in front of the breakwater is distinctively larger than the velocities measured inside the structure. This has to do with the flow of the water above the breakwater especially for submergence factors greater than zero. It can be assumed that the water flow via the pores of the structure is less than the flow above it mainly because of the difference in the permeability of the two mediums. It is interesting to notice that for zero submergence (zone R_c=0) particle velocity has almost the same value as the front face velocity (v_1), this latter validates the previous statement.

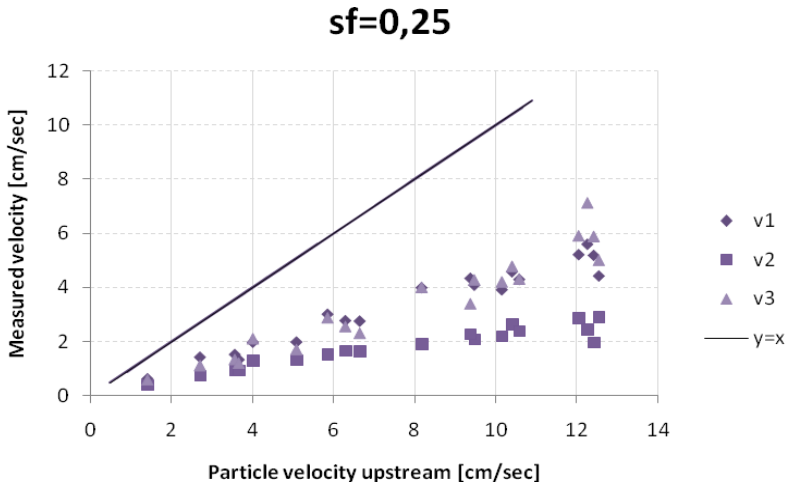

Figure 4.4.2 Calculated velocities as a function of RMS measured for s.f. =0.25

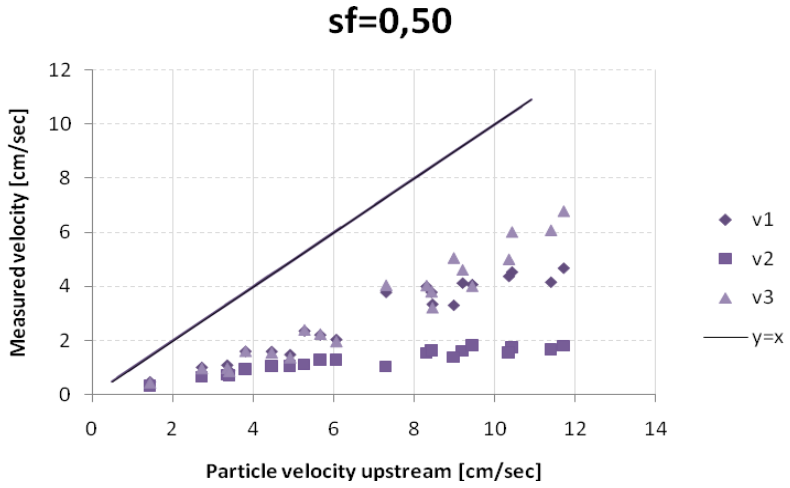

Figure 4.4.3 Calculated velocities as a function of RMS measured for s.f. =0.50

What it also needs to be discussed is the physical reasoning for large velocities occurring at the back of the breakwater, considering that the purpose of the structure is to reduce and improve the wave climate. Considering this fact, it has to be mentioned that this fact is local and it mainly occurs due to turbulence caused by the change of medium. So when the phenomenon is studied in a larger scale the technical function of the breakwater is not affected.

4.2.3. Flow velocity derived from pressure gradients

As for figures 4.5.1 and 4.5.2 velocity v_1 is much more representative for the water flow that occurs in the front face of the breakwater. Submergence doesn't affect the velocities nearly. In both cases flow velocities and measured velocities are very close.

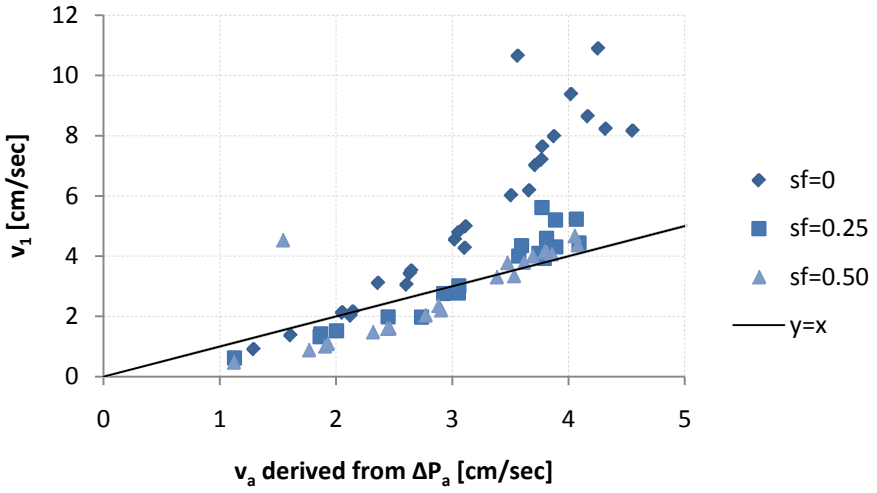

Figure 4.5.1 Flow velocity at the front face as a function of v_1.

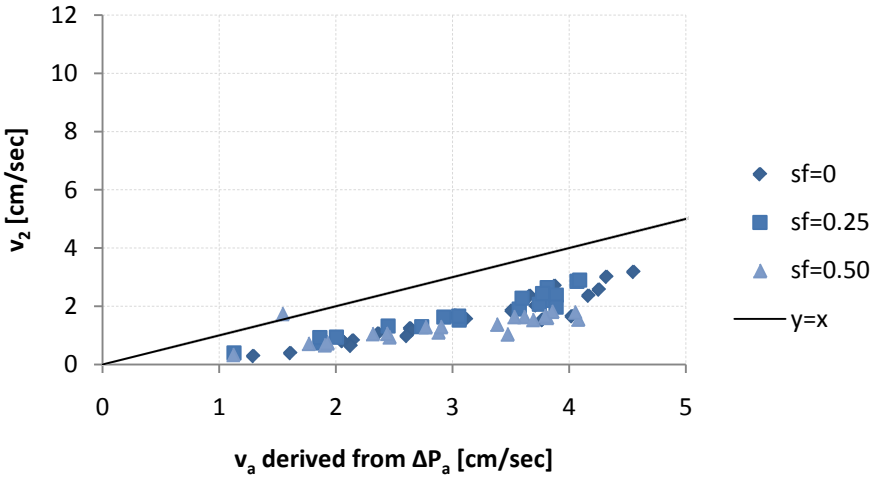

Figure 4.5.2 Flow velocity at the front face as a function of v_2.

Next two figures show that submergence is more important at the back face rather than at the front. There is on figure 4.5.4 a large difference between zero submergence and submergence greater than zero. This of course has to do with turbulence caused in zone b when submergence is above zero and with the energy loss that occurs at the front face for b=0.

Overall, it is interesting that for given permeability k=0.1m/sec measured and flow velocities are quite close to the y=x line.

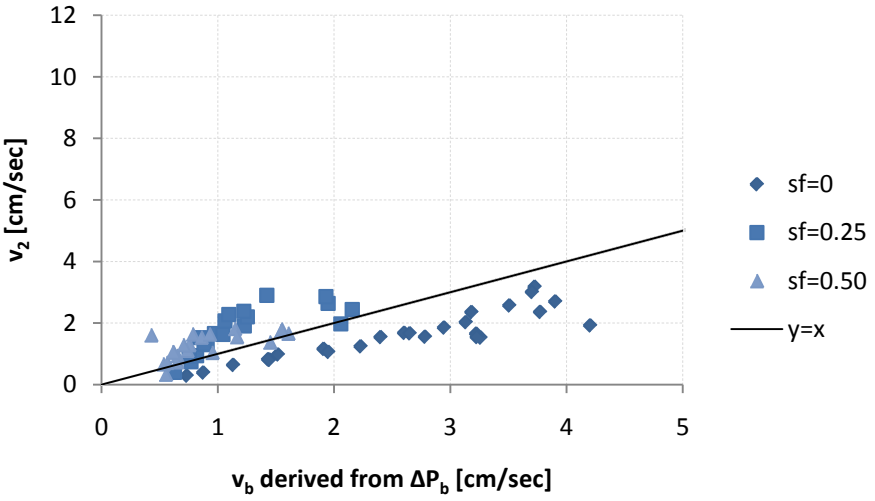

Figure 4.5.3 Flow velocity at the back face as a function of v_2.

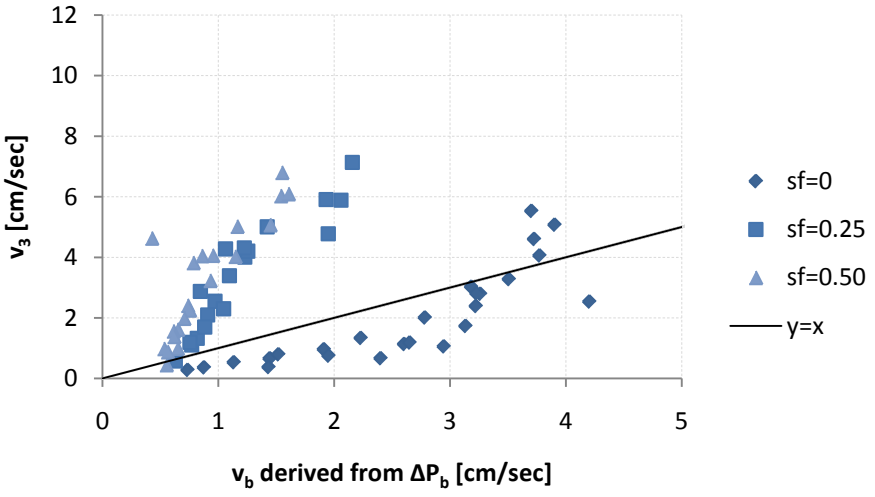

Figure 4.5.4 Flow velocity at the back face as a function of v_3.

4.3. Pressure gradients inside the breakwater

Not only measured velocities inside a rubble-mound breakwater but also pressure differences and thus flow can give interesting information about the flow that occurs inside a breakwater. Also, it is important that the data that come for the velocity meters and those that derive from the pressure meters are compared and contrasted so that out coming results are verified in this way.

4.3.1. Wave period

The following graphs clearly show the influence of the wave period over the pressure gradients inside a submerged rubble-mound breakwater. As in figure 4.6.1, the ratio $\Delta P_b/\Delta P_a$ rises as waves become longer in zero submergence conditions, while it seems that for bigger submergence factors the ratio has no influence on the wave period. This has to do mainly with the absence of the upper zone (R_c zone) when sf=0 so the water can only pass through the pores and thus its characteristics change. But, it also means that the waves break at the front face of the structure and so there is some energy loss. Generally, for sf=0.25 and sf=0.50 it seems that $\Delta P_b<\Delta P_a$, while for zero submergence it can also be $\Delta P_b=\Delta P_a$ for longer waves. This again occurs because longer waves are more resistant and therefore not a lot of energy is dissipated when long waves interact with the structure.

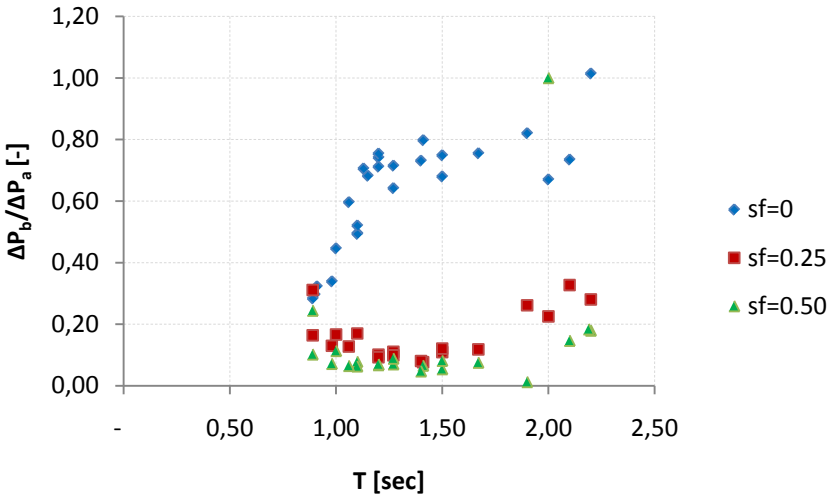

Figure 4.6.1 Wave period as a function of the ratio $\Delta P_b/\Delta P_a$

When the pressure gradients are studied indipentently and not as a ratio it is concluded that the pressure difference rising along with the wave period (Figure 4.6.2) while for the back face of the structure (Figure 4.6.3) the pressure gradient is almost not affected by the change of the period.

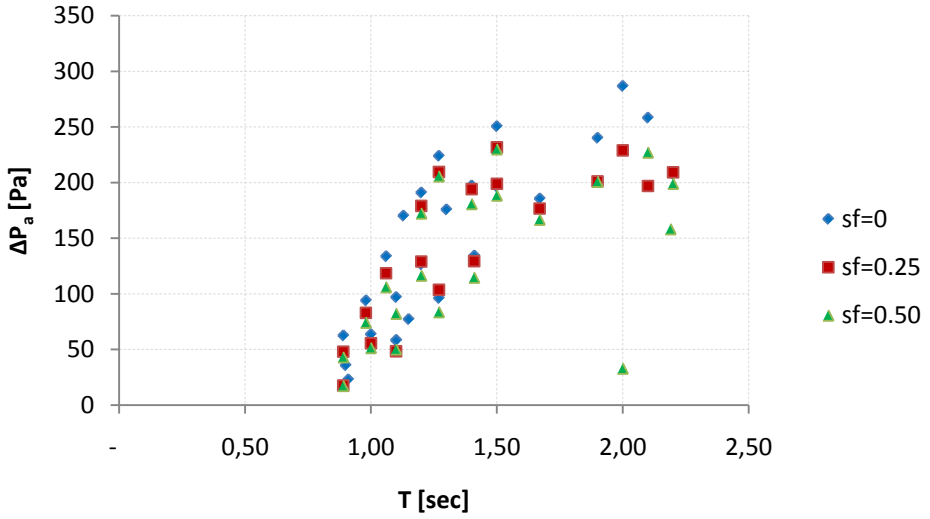

Figure 4.6.2 Wave period as a function of ΔP_a

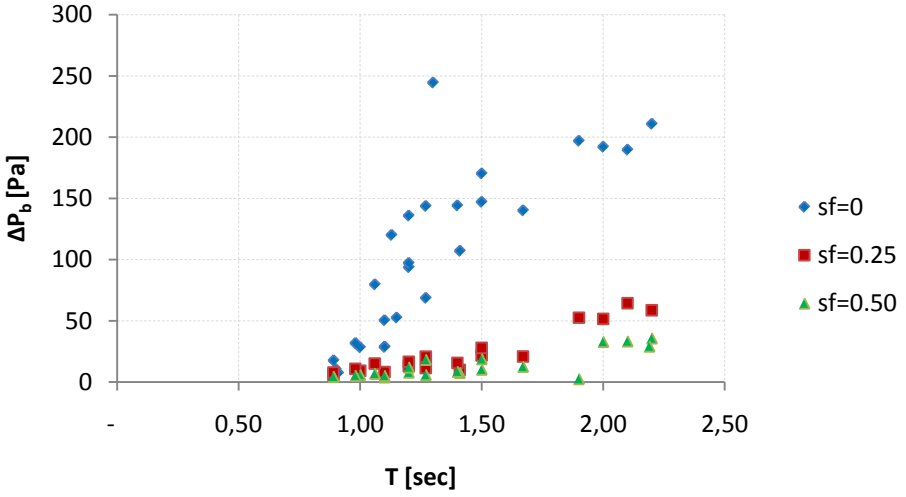

Figure 4.6.3 Wave period as a function of ΔP_b

4.3.2. Wave height

As for the figure 4.7.1, wave height seems to have almost no influence on the ratio which means that mainly submergence affects the value of the ratio which is constant for different wave heights. The ratio stays constant for constant submergence factors and the value of the ratio rises as submergence gets closer to zero. $\Delta P_b/\Delta P_a=1$ occurs for zero submergence which means that it can be assumed that the pressure gradient stays constant across the breakwater and it is not affected by the wave heights.

But when ΔP_a and ΔP_b (Figures 4.7.2 and 4.7.3) are studied individually we see that ΔP_a rises along with the wave height and in fact the slope of the trend is almost the same for every submergence factor, while in ΔP_b it is almost constant for sf>0 and rising for sf=0. Once again here sf=0 and sf>0 are considered as two different categories.

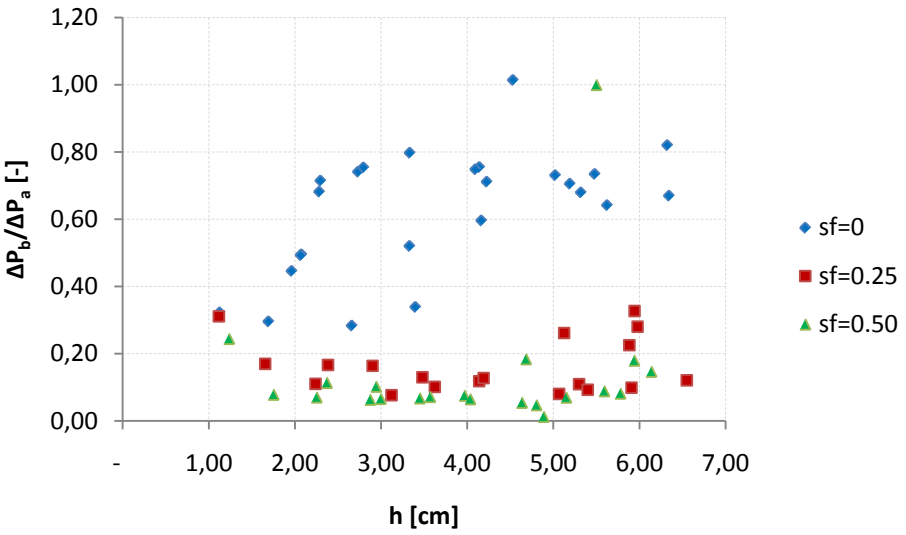

Figure 4.7.1 Wave height as a function of $\Delta P_b/\Delta P_a$

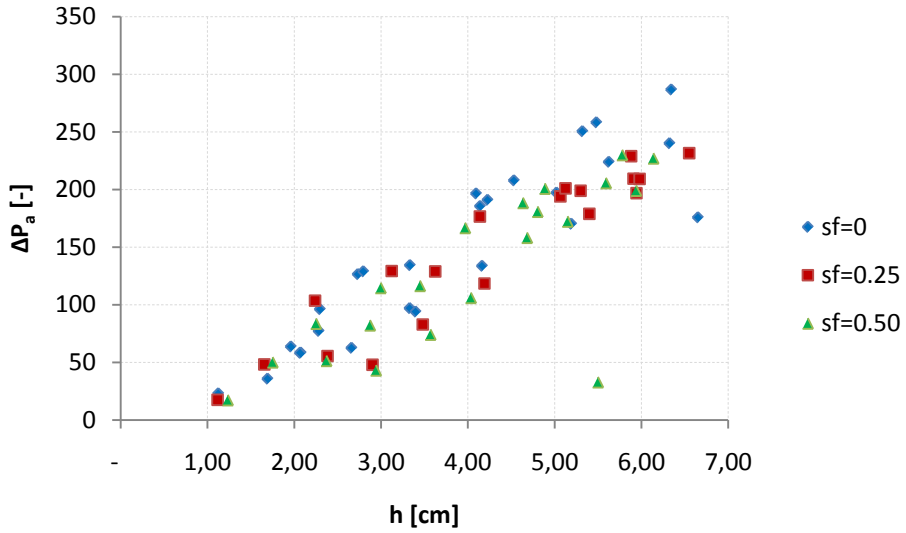

Figure 4.7.2 Wave height as a function of ΔP_a

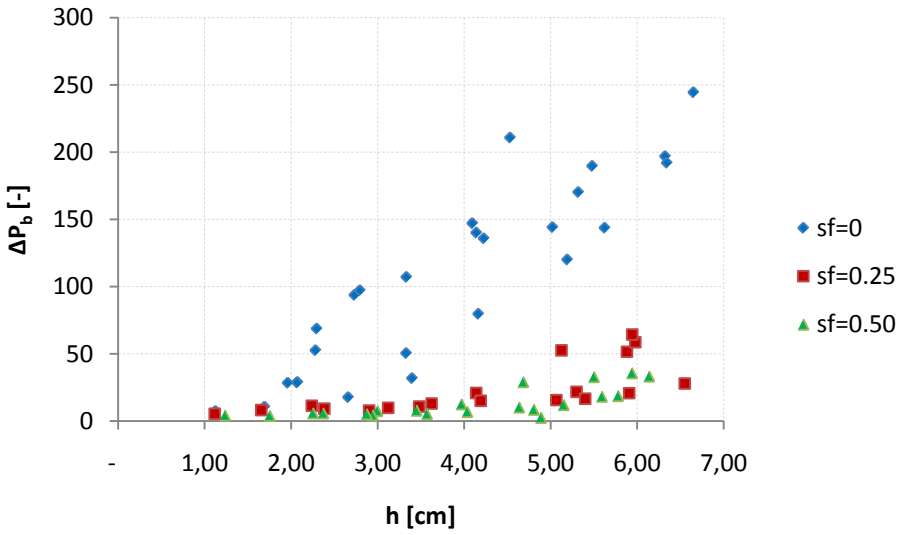

Figure 4.7.3 Wave height as a function of ΔP_b

4.3.3. Velocities and pressure gradients

4.3.3.1. At the front face of the breakwater

Figures 4.8.1, 4.8.2 and 4.8.3 show the relation between velocities inside the breakwater over pressure gradient at the front part of the structure for different submergence factors.

As for figure 4.8.1, the larger the submergence factor becomes the steeper the trend slope becomes. This means that for larger submergences, smaller pressure gradients occur because of the flow of the water above the structure (Rc zone).

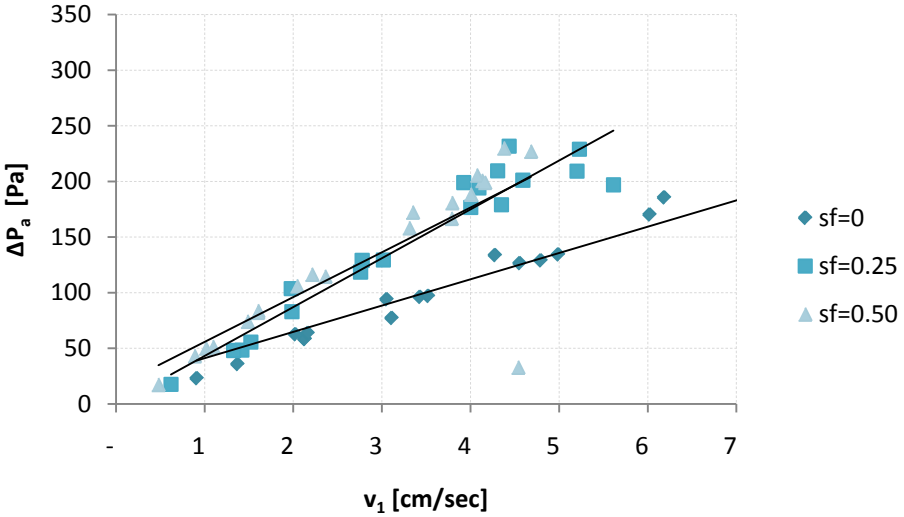

Figure 4.8.1 Velocity v_1 over ΔP_a

Figure 4.8.2 it is clear that submergence here has no influence. Velocity v_2 is the same for all submergences and it has relatively low values compared to v_1 and v_3.

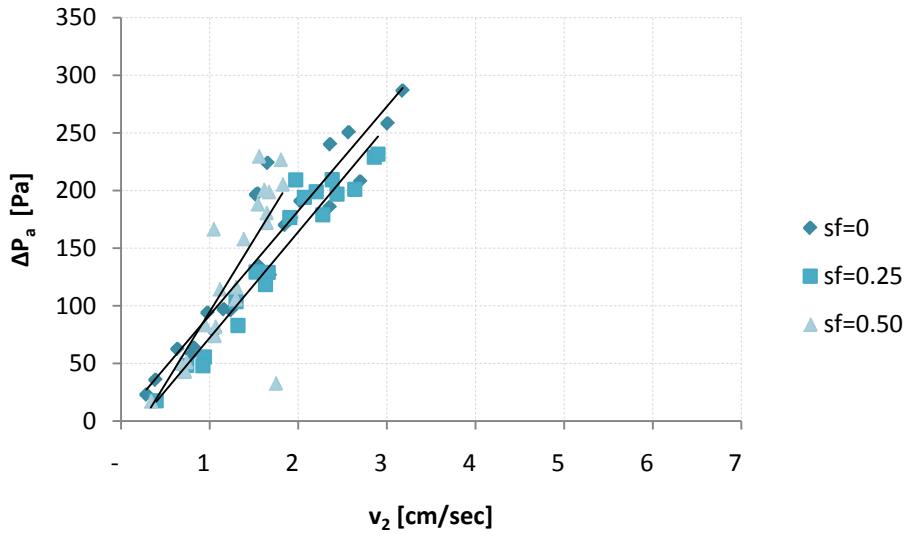

Figure 4.8.2 Velocity v_2 over ΔP_a

4.3.3.2. At the back face of the breakwater

Figure 4.9.1 shows that larger submergences lead to smaller pressure gradients because of the flow of the water above the breakwater. What is interesting to see here is the large difference on the values for sf=0 and sf>0, which validated the above statement.

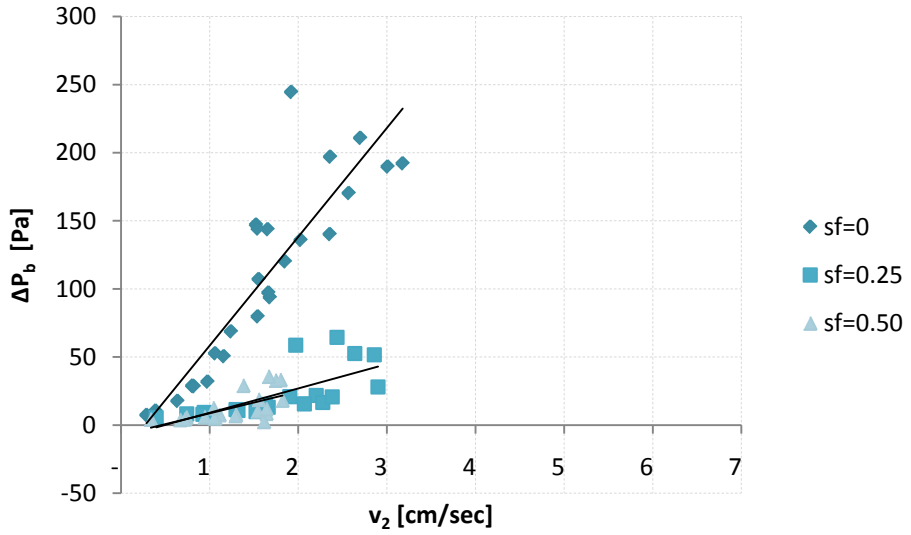

Figure 4.9.1 Velocity v_2 over ΔP_b

As for Figure 4.9.2, smaller pressure gradients occur for bigger submergences. The physical reasoning behind this is the flow of the water above the structure when sf>0 rather than via the pores of the breakwater. Here again, sf=0 and sf>0 are considered different categories.

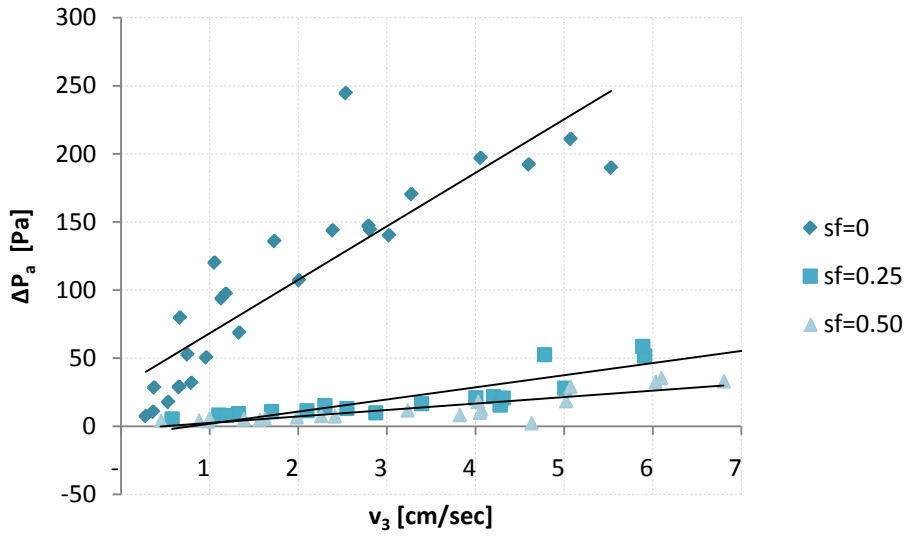

Figure 4.9.2 Velocity v_2 over ΔP_b

4.3.4. Dimensionless analysis

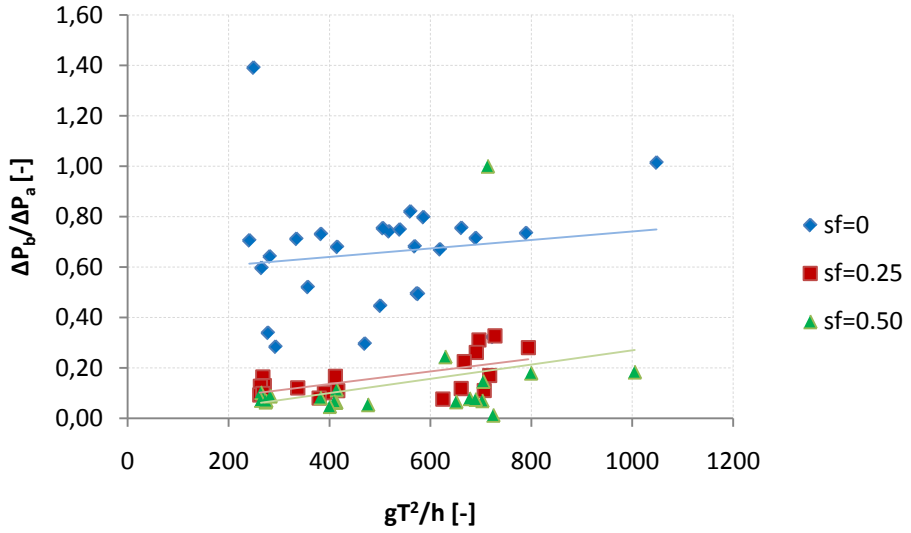

Figure 4.10 Variation of $\Delta P_b/\Delta P_a$

Figure 4.10 shows a central finding of this research. Every submergence factor corresponds to a certain ratio between ΔP_b and ΔP_a. This ratio is almost constant (slightly rising) as the gt2/h rising. In every case $\Delta P_b/\Delta P_a$ ratio is always smaller than 1, which of course means that in every case, pressure gradient at the front half of the breakwater is always larger that this at the back half of the structure. Moreover, it is interesting to see that while submergence factor rises the $\Delta P_b/\Delta P_a$ ratio decreases its value, as the R_c zone becomes higher this way and thus water moves via this zone too.

5 CONCLUSIONS AND RECOMMENDATIONS

5.1. Conclusions

The detailed conclusions of the analysis are summarized at the end of each sub-chapter of Chapter 4. The most important of them are written below.

5.1.1. Velocities inside the breakwater

The size of the voids influences intensely the local velocities that occur inside the pores of the breakwater. This means than porosity defines the difference between flow velocity and real local velocity. Considering the sea flora and fauna we need relatively high flow velocity for the renewal of the water inside the structure and thus the oxygen but quite low local velocity. So not only we need high porosity but also porosity that does not vary much from area to area.

Moreover, the characteristics of the waves play in important role on the velocities. Longer waves lead to larger velocities along the breakwater. Long waves are more resistant and carry more mass and volume.

Submergence affects the velocities that occur along the breakwater and especially the velocities at the front face, mainly because and the breaking of the waves at that area (especially for zero submergence factors) and thus the turbulence occurred. It is not strange when velocities differ a lot for zero submergence factors compared to velocities for submergence factors greater that zero as the breaking or transmitting of the wave affects the values of the velocities as well.

Particle velocity in front of the breakwater is always larger than the velocity inside the pores because of the change of the medium and thus the change of the permeability. Additionally, for submergence factors larger than zero this difference between particle velocity upstream and pore velocity become even higher. The physical reasoning behind this is that submergence factors larger than zero create a zone of water above the structure so it can be said that there is also flow of water above the breakwater rather than only via the pores, which happens for zero submergence factors.

5.1.2. Pressure gradients inside the breakwater

Pressure gradients are closely connected to the velocities inside the breakwater for specific permeability of the medium and even though the flow is turbulent. This connection between pressure gradients and velocities can differ a lot depending on whether there is zero or greater than zero submergence factor at the structure.

Pressure differences are affected by the characteristics of the wave such as wave height and wave period. Pressure difference at the front part of the breakwater rising along with the wave height or wave period while, for the back part of the structure it is that pressure gradient and almost constant and not affected by these parameters.

Last but not least, the ratio between the pressure gradients $\Delta P_b/\Delta P_a$ is almost constant (slightly rising) for every specific submergence factor and it is not affected by the dimensionless ratio gT^2/h. In every case pressure gradient at the back of the breakwater ΔP_b is always smaller than the pressure gradient at the front ΔP_a.

5.2. Recommendations

The results of this research lead to some important recommendations which are listed below.

5.2.1. Application of conclusions

The conclusions of this thesis are only applicable for a specific situation equal to the applied prototype and conditions. Expanding the validation of the relation between the parameters by executing experiments outside the range chosen is useful to increase the appropriateness of the relations on practice.

Further investigation needs to be done on the environmental part of this research

5.2.2. Influencing parameters

Various influencing parameters have not taken into consideration in this research. Their influence on the wave kinematics inside a breakwater must be investigated to define a method for calculating velocities inside such a structure. Some of the parameters that have not been varied are:

- Slope angle
- Crest width
- Stone size and porosity (local and average)
- Berm
- Wind
- Damage level

Moreover, parameters that have been taken into account in this research need more investigation of determine their exact influence on the velocities and generally water flow inside a breakwater. These parameters are:

- Water depth/ submergence factor
- Irregular wave spectrum
- More measuring points horizontically as well as vertically.

5.2.3. Scale and model effects

In the entire research, a major issue which concerns the accuracy of the final outcome is the scale and model effects. Scaling process results in scale models simulate adequately the reality. However, there are phenomena which may affect the entire process, that are not considered properly on scaling process. Conducting large scale experiments, including marine life would also be a nice idea.

This is the case for model affects also. In the analysis performed in this research, the main issue concerning the accuracy of the model was that the wave generator had limited functions and range. This consists of a model effect and further research should be conducted to neutralize the impact of such effects.

6 REFERENCES

Burcharth, H.F.; Andersen, O.H. [1993] On the one-dimensional steady and unsteady porous flow equations

Burcharth, H.F.; Liu, Z.; Troch, P. [1999] Scaling of core material in rubble mound breakwater model tests

CIRIA; CUR; CETMEF [2007] The Rock Manual. The use of rock in hydraulic engineering

Eversdijk, M. [2005] Perched beach with submerged breakwater as a solution for the shore protection for Maasvlakte ||

Hughes, S.A. [1993] Physical models and laboratory techniques in coastal engineering

Lioutas, A.; [2010] Experimental research on spatial distribution of overtopping

Pilarczyk, K.W. [1990] Coastal Protection

Pilarczyk, K.W.; Zeidler, R.B. [1996] Offshore breakwaters and shore evolution control

Schiereck, G.J. [2003] Introduction to bed, bank and shore protection

van der Meer, J.W. [1991] Stability and transmission at low-crested structures

van Gent, M.R.A. [1992] Formulae to describe porous flow

Verhagen, H.J.; d' Angermond, K.; van Roode, F.C. [2009] Breakwaters and closure dams

Zimmerman, C.; Dean, R.G.; Penchev, V. [2005] Environmental friendly coastal protection

APPENDIX

A1. Physical Model

A1.1 Photos

Photo A.1. Breakwater slope close-up

Photo A.2. Velocity transducer and pressure meter close-up

Photo A.3. Velocity transducer and pressure meter close-up

It can be seen that the distance between them is quite small.

Photo A.4. Reflection absorber

Photo A.5. Velocity transducer close-up

Photo A.6. Velocity transducer close-up

A1.2 Some more graphs

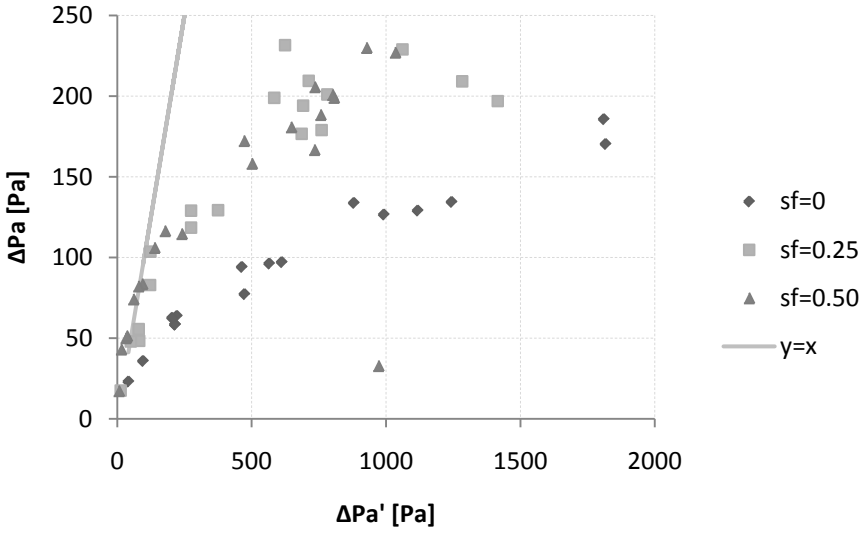

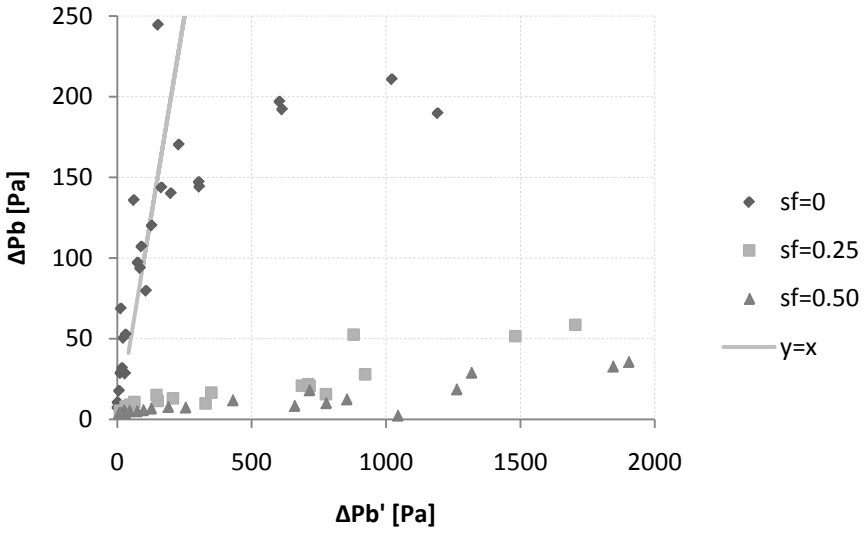

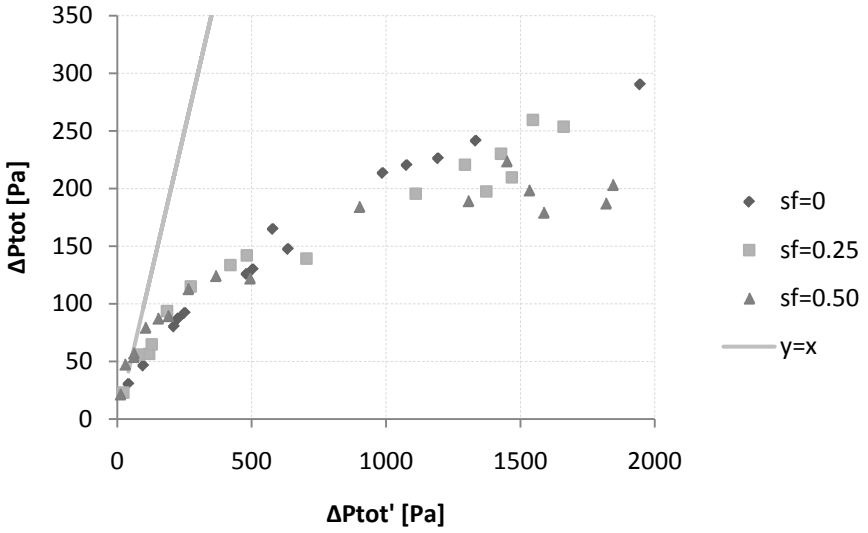

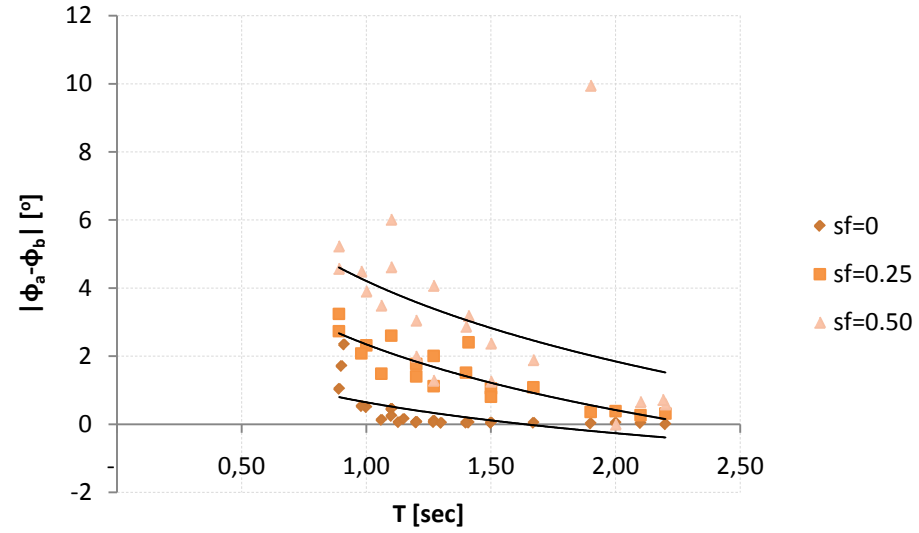
12
10
8
6
4
2
0
-2
0,50
1,00
1,50
2,00
2,50
T [sec]
|Φa-Φb| [º]
sf=0
sf=0.25
sf=0.50

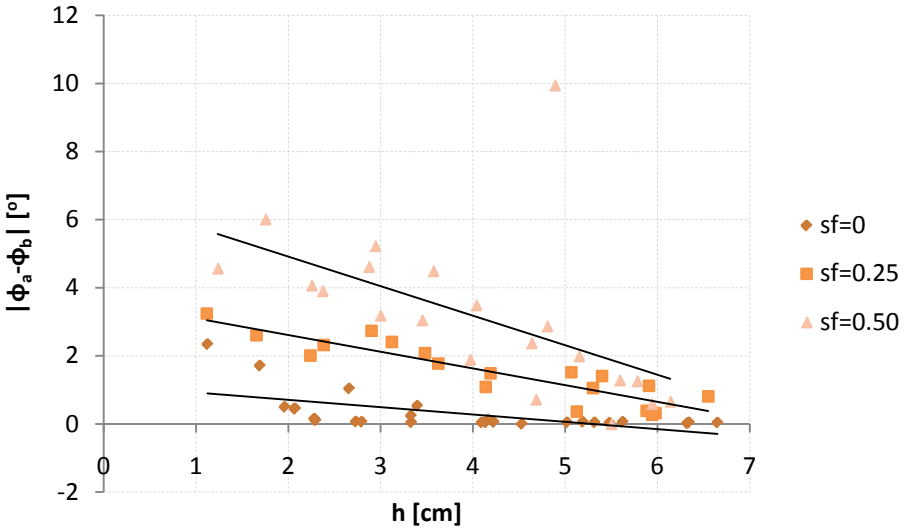
12
10
8
6
4
2
0
-2
0
1
2
3
4
5
6
7
h [cm]
|Φa-Φb| [º]
sf=0
sf=0.25
sf=0.50

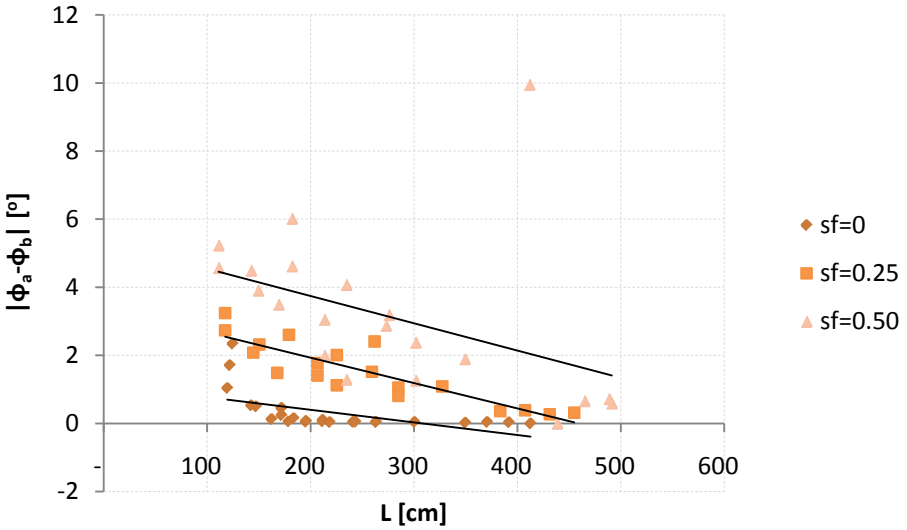
12
10
8
6
4
2
0
-2
100
200
300
400
500
600
L [cm]
|Φa-Φb| [º]
sf=0
sf=0.25
sf=0.50

A1.3 Measuring data and computations

A1.3.1 Velocities

No	d [cm]	T [sec]	h1 [cm]	h2 [cm]	v1 [cm/s]	v2 [cm/s]	v3 [cm/s]	ΔP_b [Pa]	ΔP_a [Pa]	D_{n50}/h	$\lvert v_1-v_3 \rvert$ [cm/sec]
53	40	0,91	1,12	0,18	0,91	0,29	0,28	7,45	23,08	6,50	0,63
54	40	1,10	2,07	0,38	2,13	0,80	0,65	28,94	58,42	3,52	1,47
55	40	1,10	2,07	0,38	2,13	0,81	0,66	28,78	58,37	3,53	1,47
56	40	0,90	1,69	0,34	1,37	0,39	0,36	10,60	35,83	4,32	1,01
57	40	1,27	2,30	0,57	3,43	1,24	1,33	68,76	96,20	3,18	2,09
58	40	1,00	1,96	0,50	2,16	0,82	0,37	28,43	63,74	3,72	1,79
59	40	1,41	3,33	0,99	4,99	1,55	2,01	107,17	134,37	2,19	2,98
60	40	0,89	2,66	0,52	2,02	0,64	0,53	17,75	62,60	2,75	1,49
61	40	1,10	3,33	0,63	3,52	1,16	0,96	50,51	97,07	2,19	2,56
62	40	0,98	3,40	0,72	3,05	0,98	0,79	31,89	94,07	2,15	2,26
63	40	1,20	2,73	0,91	4,55	1,68	1,13	93,81	126,55	2,67	3,42
64	40	1,67	4,14	1,56	6,18	2,35	3,02	140,18	185,65	1,76	3,16
65	40	1,06	4,16	1,07	4,27	1,54	0,67	79,75	133,76	1,75	3,61
66	40	1,13	5,19	1,56	6,02	1,85	1,06	120,13	170,26	1,41	4,96
67	40	1,90	6,32	2,22	8,64	2,36	4,06	197,00	240,18	1,15	4,59
68	40	1,20	4,23	1,41	7,02	2,03	1,73	135,91	191,02	1,73	5,29
69	40	2,00	6,34	2,77	8,17	3,18	4,60	192,12	286,77	1,15	3,56
70	40	1,27	5,62	1,87	9,38	1,65	2,39	143,76	224,00	1,30	6,99
83	40	1,15	2,28	0,64	3,11	1,06	0,75	52,68	77,26	3,20	2,36
84	40	1,20	2,79	0,89	4,79	1,66	1,18	97,27	129,01	2,61	3,61
85	40	1,50	4,09	1,72	7,20	1,52	2,79	147,15	196,58	1,78	4,41
86	40	1,40	5,02	1,73	7,64	1,54	2,81	144,23	197,32	1,45	4,83
87	40	2,20	4,53	3,05	7,98	2,70	5,07	210,83	207,92	1,61	2,91
88	40	1,50	5,32	2,21	10,90	2,57	3,28	170,32	250,60	1,37	7,62
89	40	2,10	5,48	2,80	8,23	3,01	5,53	189,75	258,32	1,33	2,70
90	40	1,30	6,65	1,87	10,65	1,92	2,54	244,52	175,84	1,10	8,12
102	50	0,89	1,12	1,18	0,62	0,40	0,58	5,46	17,56	6,54	0,04
103	50	1,10	1,65	1,67	1,42	0,74	1,10	8,21	48,33	4,41	0,32
104	50	1,27	2,24	2,23	1,98	1,30	2,10	11,42	103,64	3,26	0,12
105	50	1,00	2,38	1,92	1,52	0,94	1,33	9,26	55,61	3,06	0,20
106	50	1,41	3,12	2,56	3,02	1,52	2,87	9,88	129,33	2,34	0,14
107	50	0,89	2,90	2,63	1,33	0,92	1,19	7,87	48,02	2,52	0,13
108	50	1,20	3,62	2,94	2,78	1,66	2,55	13,06	129,01	2,01	0,23
109	50	0,98	3,48	3,02	1,98	1,32	1,70	10,77	82,95	2,10	0,29
110	50	1,67	4,14	3,15	4,00	1,90	4,00	20,89	176,65	1,76	0,00
111	50	1,06	4,19	3,27	2,76	1,63	2,30	15,12	118,49	1,74	0,46
112	50	1,50	5,30	3,88	3,92	2,20	4,20	21,78	198,94	1,38	0,28
113	50	1,40	5,07	4,17	4,09	2,07	4,28	15,62	194,11	1,44	0,18
114	50	1,90	5,13	4,15	4,59	2,64	4,78	52,57	201,08	1,42	0,19
115	50	1,20	5,40	4,31	4,35	2,28	3,39	16,61	178,98	1,35	0,96
116	50	2,00	5,88	4,71	5,23	2,86	5,91	51,59	228,98	1,24	0,68
117	50	1,27	5,91	5,06	4,31	2,38	4,31	20,74	209,47	1,24	0,01
118	50	2,20	5,98	5,27	5,20	1,97	5,89	58,65	209,22	1,22	0,69
119	50	1,50	6,55	4,87	4,44	2,90	5,01	27,98	231,62	1,11	0,57
120	50	2,10	5,94	5,88	5,61	2,44	7,13	64,41	196,92	1,23	1,52
124	60	0,89	1,23	1,11	0,48	0,34	0,45	4,24	17,35	5,91	0,03
125	60	1,10	1,75	1,62	1,01	0,67	0,98	3,93	50,15	4,17	0,03
126	60	1,27	2,25	2,07	1,60	0,94	1,62	5,87	83,65	3,24	0,01
127	60	1,00	2,37	2,19	1,10	0,74	0,99	5,84	51,42	3,08	0,10
128	60	1,41	3,00	2,57	2,36	1,11	2,41	7,54	114,66	2,44	0,05
130	60	0,89	2,94	2,80	0,89	0,72	0,88	4,41	43,13	2,48	0,01
131	60	1,10	2,87	2,65	1,60	1,06	1,56	5,21	82,22	2,54	0,04
132	60	0,98	3,57	3,24	1,48	1,05	1,38	5,31	74,18	2,04	0,10
133	60	1,20	3,45	3,12	2,21	1,30	2,25	7,87	116,47	2,12	0,04
134	60	1,67	3,97	3,44	3,79	1,04	4,06	12,59	166,73	1,84	0,27

135	60	1,06	4,04	3,65	2,04	1,29	1,98	6,89	106,08	1,81	0,06
136	60	1,40	4,80	4,12	3,79	1,64	3,82	8,54	180,81	1,52	0,03
137	60	1,50	4,64	4,09	4,00	1,54	4,05	10,24	188,42	1,57	0,04
138	60	1,90	4,89	4,43	4,13	1,61	4,63	2,53	200,83	1,49	0,50
139	60	1,20	5,15	4,50	3,35	1,64	3,23	12,01	172,31	1,42	0,12
140	60	2,00	5,50	4,95	4,54	1,74	6,03	32,89	32,89	1,33	1,49
141	60	1,27	5,59	5,00	4,07	1,82	4,03	18,24	205,66	1,31	0,05
142	60	1,50	5,78	5,10	4,38	1,55	5,02	18,78	229,99	1,26	0,64
143	60	2,20	5,94	5,08	4,16	1,67	6,09	35,76	199,05	1,23	1,93
144	60	2,10	6,14	5,71	4,68	1,80	6,80	33,31	227,06	1,19	2,12
145	60	2,19	4,68	4,05	3,31	1,38	5,07	29,10	158,21	1,56	1,76

$\lvert v_1-v_2\rvert$ [cm/sec]	$\lvert v_2-v_3\rvert$ [cm/sec]	Visser's L_0 [cm]	Visser's L [cm]	α	ω	k	z+d	d	u [cm/sec]
0,62	0,01	129,24	124,50	0,01	6,90	5,05	0,20	0,40	1,630
1,32	0,15	188,97	171,87	0,01	5,71	3,66	0,20	0,40	3,709
1,32	0,15	189,00	171,89	0,01	5,71	3,66	0,20	0,40	3,695
0,98	0,03	126,36	121,85	0,01	6,98	5,16	0,20	0,40	2,411
2,19	0,09	251,73	211,65	0,01	4,95	2,97	0,20	0,40	4,510
1,34	0,45	156,00	147,30	0,01	6,28	4,27	0,20	0,40	3,206
3,43	0,46	310,45	243,44	0,02	4,45	2,58	0,20	0,40	6,878
1,38	0,10	123,82	119,47	0,01	7,05	5,26	0,20	0,40	3,730
2,36	0,20	188,90	171,82	0,02	5,71	3,66	0,20	0,40	5,953
2,08	0,18	150,04	142,48	0,02	6,41	4,41	0,20	0,40	5,436
2,87	0,54	224,83	195,50	0,01	5,23	3,21	0,20	0,40	5,195
3,83	0,67	435,38	300,53	0,02	3,76	2,09	0,20	0,40	9,044
2,73	0,88	175,51	162,23	0,02	5,92	3,87	0,20	0,40	7,215
4,17	0,80	198,91	178,70	0,03	5,56	3,52	0,20	0,40	9,469
6,28	1,70	563,16	349,64	0,03	3,31	1,80	0,20	0,40	14,235
5,00	0,30	224,64	195,38	0,02	5,24	3,22	0,20	0,40	8,035
4,99	1,42	624,00	370,79	0,03	3,14	1,69	0,20	0,40	14,420
7,73	0,73	251,61	211,58	0,03	4,95	2,97	0,20	0,40	11,049
2,05	0,31	206,31	183,64	0,01	5,46	3,42	0,20	0,40	4,216
3,13	0,48	224,64	195,38	0,01	5,24	3,22	0,20	0,40	5,313
5,68	1,27	351,00	263,27	0,02	4,19	2,39	0,20	0,40	8,650
6,10	1,27	305,76	241,05	0,03	4,49	2,61	0,20	0,40	10,332
5,28	2,37	755,04	412,71	0,02	2,86	1,52	0,20	0,40	10,461
8,33	0,71	351,00	263,27	0,03	4,19	2,39	0,20	0,40	11,238
5,22	2,52	687,96	391,80	0,03	2,99	1,60	0,20	0,40	12,563
8,73	0,62	263,64	218,45	0,03	4,83	2,88	0,20	0,40	13,226
0,22	0,18	123,57	117,35	0,01	7,06	5,35	0,30	0,50	1,411
0,68	0,36	188,76	179,09	0,01	5,71	3,51	0,30	0,50	2,709
0,68	0,80	251,61	225,38	0,01	4,95	2,79	0,30	0,50	4,014
0,58	0,39	156,00	150,49	0,01	6,28	4,18	0,30	0,50	3,569
1,49	1,35	310,14	261,93	0,02	4,46	2,40	0,30	0,50	5,859
0,40	0,27	123,57	117,35	0,01	7,06	5,35	0,30	0,50	3,669
1,12	0,89	224,64	206,61	0,02	5,24	3,04	0,30	0,50	6,299
0,67	0,38	149,82	144,61	0,02	6,41	4,34	0,30	0,50	5,090
2,10	2,10	435,07	327,35	0,02	3,76	1,92	0,30	0,50	8,181
1,13	0,67	175,28	167,79	0,02	5,93	3,74	0,30	0,50	6,652
1,72	2,00	351,00	284,89	0,03	4,19	2,21	0,30	0,50	10,162
2,03	2,21	305,76	259,36	0,03	4,49	2,42	0,30	0,50	9,481
1,95	2,14	563,16	383,44	0,03	3,31	1,64	0,30	0,50	10,414
2,07	1,12	224,64	206,61	0,03	5,24	3,04	0,30	0,50	9,384
2,37	3,05	624,00	407,45	0,03	3,14	1,54	0,30	0,50	12,058
1,92	1,93	251,61	225,38	0,03	4,95	2,79	0,30	0,50	10,591
3,23	3,92	755,04	454,97	0,03	2,86	1,38	0,30	0,50	12,429
1,54	2,11	351,00	284,89	0,03	4,19	2,21	0,30	0,50	12,559
3,18	4,70	687,96	431,29	0,03	2,99	1,46	0,30	0,50	12,275
0,14	0,11	123,57	111,08	0,01	7,06	5,66	0,40	0,60	1,423
0,35	0,31	188,76	182,04	0,01	5,71	3,45	0,40	0,60	2,709
0,66	0,68	251,61	234,64	0,01	4,95	2,68	0,40	0,60	3,795
0,36	0,26	156,00	149,30	0,01	6,28	4,21	0,40	0,60	3,341

1,25	1,30	310,14	275,90	0,01	4,46	2,28	0,40	0,60	5,260
0,17	0,16	123,57	111,08	0,01	7,06	5,66	0,40	0,60	3,390
0,54	0,50	188,76	182,04	0,01	5,71	3,45	0,40	0,60	4,445
0,43	0,33	149,82	142,54	0,02	6,41	4,41	0,40	0,60	4,903
0,92	0,96	224,64	213,37	0,02	5,24	2,94	0,40	0,60	5,650
2,74	3,02	435,07	349,28	0,02	3,76	1,80	0,40	0,60	7,287
0,75	0,69	175,28	169,14	0,02	5,93	3,71	0,40	0,60	6,051
2,15	2,18	305,76	273,00	0,02	4,49	2,30	0,40	0,60	8,414
2,47	2,51	351,00	301,71	0,02	4,19	2,08	0,40	0,60	8,292
2,52	3,02	563,16	411,85	0,02	3,31	1,53	0,40	0,60	9,187
1,71	1,59	224,64	213,37	0,03	5,24	2,94	0,40	0,60	8,437
2,79	4,28	624,00	438,57	0,03	3,14	1,43	0,40	0,60	10,415
2,25	2,20	251,61	234,64	0,03	4,95	2,68	0,40	0,60	9,426
2,82	3,47	351,00	301,71	0,03	4,19	2,08	0,40	0,60	10,338
2,50	4,43	755,04	491,33	0,03	2,86	1,28	0,40	0,60	11,382
2,88	5,00	687,96	465,05	0,03	2,99	1,35	0,40	0,60	11,698
1,93	3,69	748,19	488,71	0,02	2,87	1,29	0,40	0,60	8,968

$\lvert v_1-v_2\rvert$ [cm/sec]	$\lvert v_2-v_3\rvert$ [cm/sec]	Visser's L_0 [cm]	Visser's L [cm]	α	ω	k	z+d	d	u [cm/sec]
0,62	0,01	129,24	124,50	0,01	6,90	5,05	0,20	0,40	1,630
1,32	0,15	188,97	171,87	0,01	5,71	3,66	0,20	0,40	3,709
1,32	0,15	189,00	171,89	0,01	5,71	3,66	0,20	0,40	3,695
0,98	0,03	126,36	121,85	0,01	6,98	5,16	0,20	0,40	2,411
2,19	0,09	251,73	211,65	0,01	4,95	2,97	0,20	0,40	4,510
1,34	0,45	156,00	147,30	0,01	6,28	4,27	0,20	0,40	3,206
3,43	0,46	310,45	243,44	0,02	4,45	2,58	0,20	0,40	6,878
1,38	0,10	123,82	119,47	0,01	7,05	5,26	0,20	0,40	3,730
2,36	0,20	188,90	171,82	0,02	5,71	3,66	0,20	0,40	5,953
2,08	0,18	150,04	142,48	0,02	6,41	4,41	0,20	0,40	5,436
2,87	0,54	224,83	195,50	0,01	5,23	3,21	0,20	0,40	5,195
3,83	0,67	435,38	300,53	0,02	3,76	2,09	0,20	0,40	9,044
2,73	0,88	175,51	162,23	0,02	5,92	3,87	0,20	0,40	7,215
4,17	0,80	198,91	178,70	0,03	5,56	3,52	0,20	0,40	9,469
6,28	1,70	563,16	349,64	0,03	3,31	1,80	0,20	0,40	14,235
5,00	0,30	224,64	195,38	0,02	5,24	3,22	0,20	0,40	8,035
4,99	1,42	624,00	370,79	0,03	3,14	1,69	0,20	0,40	14,420
7,73	0,73	251,61	211,58	0,03	4,95	2,97	0,20	0,40	11,049
2,05	0,31	206,31	183,64	0,01	5,46	3,42	0,20	0,40	4,216
3,13	0,48	224,64	195,38	0,01	5,24	3,22	0,20	0,40	5,313
5,68	1,27	351,00	263,27	0,02	4,19	2,39	0,20	0,40	8,650
6,10	1,27	305,76	241,05	0,03	4,49	2,61	0,20	0,40	10,332
5,28	2,37	755,04	412,71	0,02	2,86	1,52	0,20	0,40	10,461
8,33	0,71	351,00	263,27	0,03	4,19	2,39	0,20	0,40	11,238
5,22	2,52	687,96	391,80	0,03	2,99	1,60	0,20	0,40	12,563
8,73	0,62	263,64	218,45	0,03	4,83	2,88	0,20	0,40	13,226
0,22	0,18	123,57	117,35	0,01	7,06	5,35	0,30	0,50	1,411
0,68	0,36	188,76	179,09	0,01	5,71	3,51	0,30	0,50	2,709
0,68	0,80	251,61	225,38	0,01	4,95	2,79	0,30	0,50	4,014
0,58	0,39	156,00	150,49	0,01	6,28	4,18	0,30	0,50	3,569
1,49	1,35	310,14	261,93	0,02	4,46	2,40	0,30	0,50	5,859
0,40	0,27	123,57	117,35	0,01	7,06	5,35	0,30	0,50	3,669
1,12	0,89	224,64	206,61	0,02	5,24	3,04	0,30	0,50	6,299
0,67	0,38	149,82	144,61	0,02	6,41	4,34	0,30	0,50	5,090
2,10	2,10	435,07	327,35	0,02	3,76	1,92	0,30	0,50	8,181
1,13	0,67	175,28	167,79	0,02	5,93	3,74	0,30	0,50	6,652
1,72	2,00	351,00	284,89	0,03	4,19	2,21	0,30	0,50	10,162
2,03	2,21	305,76	259,36	0,03	4,49	2,42	0,30	0,50	9,481
1,95	2,14	563,16	383,44	0,03	3,31	1,64	0,30	0,50	10,414
2,07	1,12	224,64	206,61	0,03	5,24	3,04	0,30	0,50	9,384
2,37	3,05	624,00	407,45	0,03	3,14	1,54	0,30	0,50	12,058
1,92	1,93	251,61	225,38	0,03	4,95	2,79	0,30	0,50	10,591
3,23	3,92	755,04	454,97	0,03	2,86	1,38	0,30	0,50	12,429

1,54	2,11	351,00	284,89	0,03	4,19	2,21	0,30	0,50	12,559
3,18	4,70	687,96	431,29	0,03	2,99	1,46	0,30	0,50	12,275
0,14	0,11	123,57	111,08	0,01	7,06	5,66	0,40	0,60	1,423
0,35	0,31	188,76	182,04	0,01	5,71	3,45	0,40	0,60	2,709
0,66	0,68	251,61	234,64	0,01	4,95	2,68	0,40	0,60	3,795
0,36	0,26	156,00	149,30	0,01	6,28	4,21	0,40	0,60	3,341
1,25	1,30	310,14	275,90	0,01	4,46	2,28	0,40	0,60	5,260
0,17	0,16	123,57	111,08	0,01	7,06	5,66	0,40	0,60	3,390
0,54	0,50	188,76	182,04	0,01	5,71	3,45	0,40	0,60	4,445
0,43	0,33	149,82	142,54	0,02	6,41	4,41	0,40	0,60	4,903
0,92	0,96	224,64	213,37	0,02	5,24	2,94	0,40	0,60	5,650
2,74	3,02	435,07	349,28	0,02	3,76	1,80	0,40	0,60	7,287
0,75	0,69	175,28	169,14	0,02	5,93	3,71	0,40	0,60	6,051
2,15	2,18	305,76	273,00	0,02	4,49	2,30	0,40	0,60	8,414
2,47	2,51	351,00	301,71	0,02	4,19	2,08	0,40	0,60	8,292
2,52	3,02	563,16	411,85	0,02	3,31	1,53	0,40	0,60	9,187
1,71	1,59	224,64	213,37	0,03	5,24	2,94	0,40	0,60	8,437
2,79	4,28	624,00	438,57	0,03	3,14	1,43	0,40	0,60	10,415
2,25	2,20	251,61	234,64	0,03	4,95	2,68	0,40	0,60	9,426
2,82	3,47	351,00	301,71	0,03	4,19	2,08	0,40	0,60	10,338
2,50	4,43	755,04	491,33	0,03	2,86	1,28	0,40	0,60	11,382
2,88	5,00	687,96	465,05	0,03	2,99	1,35	0,40	0,60	11,698
1,93	3,69	748,19	488,71	0,02	2,87	1,29	0,40	0,60	8,968

A1.3.2 Pressure gradients

No	d [cm]	T [sec]	h1 [cm]	h2 [cm]	v1 [cm/s]	v2 [cm/s]	v3 [cm/s]	ΔP_b [Pa]	ΔP_a [Pa]	ΔPb/Δpa	Visser's L0 [cm]
53	40	0,91	1,12	0,18	0,91	0,29	0,28	7,45	23,08	0,32	129,24
54	40	1,10	2,07	0,38	2,13	0,80	0,65	28,94	58,42	0,50	188,97
55	40	1,10	2,07	0,38	2,13	0,81	0,66	28,78	58,37	0,49	189,00
56	40	0,90	1,69	0,34	1,37	0,39	0,36	10,60	35,83	0,30	126,36
57	40	1,27	2,30	0,57	3,43	1,24	1,33	68,76	96,20	0,71	251,73
58	40	1,00	1,96	0,50	2,16	0,82	0,37	28,43	63,74	0,45	156,00
59	40	1,41	3,33	0,99	4,99	1,55	2,01	107,17	134,37	0,80	310,45
60	40	0,89	2,66	0,52	2,02	0,64	0,53	17,75	62,60	0,28	123,82
61	40	1,10	3,33	0,63	3,52	1,16	0,96	50,51	97,07	0,52	188,90
62	40	0,98	3,40	0,72	3,05	0,98	0,79	31,89	94,07	0,34	150,04
63	40	1,20	2,73	0,91	4,55	1,68	1,13	93,81	126,55	0,74	224,83
64	40	1,67	4,14	1,56	6,18	2,35	3,02	140,18	185,65	0,76	435,38
65	40	1,06	4,16	1,07	4,27	1,54	0,67	79,75	133,76	0,60	175,51
66	40	1,13	5,19	1,56	6,02	1,85	1,06	120,13	170,26	0,71	198,91
67	40	1,90	6,32	2,22	8,64	2,36	4,06	197,00	240,18	0,82	563,16
68	40	1,20	4,23	1,41	7,02	2,03	1,73	135,91	191,02	0,71	224,64
69	40	2,00	6,34	2,77	8,17	3,18	4,60	192,12	286,77	0,67	624,00
70	40	1,27	5,62	1,87	9,38	1,65	2,39	143,76	224,00	0,64	251,61
83	40	1,15	2,28	0,64	3,11	1,06	0,75	52,68	77,26	0,68	206,31
84	40	1,20	2,79	0,89	4,79	1,66	1,18	97,27	129,01	0,75	224,64
85	40	1,50	4,09	1,72	7,20	1,52	2,79	147,15	196,58	0,75	351,00
86	40	1,40	5,02	1,73	7,64	1,54	2,81	144,23	197,32	0,73	305,76
87	40	2,20	4,53	3,05	7,98	2,70	5,07	210,83	207,92	1,01	755,04
88	40	1,50	5,32	2,21	10,90	2,57	3,28	170,32	250,60	0,68	351,00
89	40	2,10	5,48	2,80	8,23	3,01	5,53	189,75	258,32	0,73	687,96
90	40	1,30	6,65	1,87	10,65	1,92	2,54	244,52	175,84	1,39	263,64
102	50	0,89	1,12	1,18	0,62	0,40	0,58	5,46	17,56	0,31	123,57
103	50	1,10	1,65	1,67	1,42	0,74	1,10	8,21	48,33	0,17	188,76
104	50	1,27	2,24	2,23	1,98	1,30	2,10	11,42	103,64	0,11	251,61
105	50	1,00	2,38	1,92	1,52	0,94	1,33	9,26	55,61	0,17	156,00
106	50	1,41	3,12	2,56	3,02	1,52	2,87	9,88	129,33	0,08	310,14
107	50	0,89	2,90	2,63	1,33	0,92	1,19	7,87	48,02	0,16	123,57
108	50	1,20	3,62	2,94	2,78	1,66	2,55	13,06	129,01	0,10	224,64
109	50	0,98	3,48	3,02	1,98	1,32	1,70	10,77	82,95	0,13	149,82
110	50	1,67	4,14	3,15	4,00	1,90	4,00	20,89	176,65	0,12	435,07
111	50	1,06	4,19	3,27	2,76	1,63	2,30	15,12	118,49	0,13	175,28
112	50	1,50	5,30	3,88	3,92	2,20	4,20	21,78	198,94	0,11	351,00
113	50	1,40	5,07	4,17	4,09	2,07	4,28	15,62	194,11	0,08	305,76
114	50	1,90	5,13	4,15	4,59	2,64	4,78	52,57	201,08	0,26	563,16
115	50	1,20	5,40	4,31	4,35	2,28	3,39	16,61	178,98	0,09	224,64
116	50	2,00	5,88	4,71	5,23	2,86	5,91	51,59	228,98	0,23	624,00
117	50	1,27	5,91	5,06	4,31	2,38	4,31	20,74	209,47	0,10	251,61
118	50	2,20	5,98	5,27	5,20	1,97	5,89	58,65	209,22	0,28	755,04
119	50	1,50	6,55	4,87	4,44	2,90	5,01	27,98	231,62	0,12	351,00
120	50	2,10	5,94	5,88	5,61	2,44	7,13	64,41	196,92	0,33	687,96
124	60	0,89	1,23	1,11	0,48	0,34	0,45	4,24	17,35	0,24	123,57
125	60	1,10	1,75	1,62	1,01	0,67	0,98	3,93	50,15	0,08	188,76
126	60	1,27	2,25	2,07	1,60	0,94	1,62	5,87	83,65	0,07	251,61
127	60	1,00	2,37	2,19	1,10	0,74	0,99	5,84	51,42	0,11	156,00
128	60	1,41	3,00	2,57	2,36	1,11	2,41	7,54	114,66	0,07	310,14
130	60	0,89	2,94	2,80	0,89	0,72	0,88	4,41	43,13	0,10	123,57
131	60	1,10	2,87	2,65	1,60	1,06	1,56	5,21	82,22	0,06	188,76
132	60	0,98	3,57	3,24	1,48	1,05	1,38	5,31	74,18	0,07	149,82
133	60	1,20	3,45	3,12	2,21	1,30	2,25	7,87	116,47	0,07	224,64
134	60	1,67	3,97	3,44	3,79	1,04	4,06	12,59	166,73	0,08	435,07
135	60	1,06	4,04	3,65	2,04	1,29	1,98	6,89	106,08	0,06	175,28
136	60	1,40	4,80	4,12	3,79	1,64	3,82	8,54	180,81	0,05	305,76
137	60	1,50	4,64	4,09	4,00	1,54	4,05	10,24	188,42	0,05	351,00

138	60	1,90	4,89	4,43	4,13	1,61	4,63	2,53	200,83	0,01	563,16
139	60	1,20	5,15	4,50	3,35	1,64	3,23	12,01	172,31	0,07	224,64
140	60	2,00	5,50	4,95	4,54	1,74	6,03	32,89	32,89	1,00	624,00
141	60	1,27	5,59	5,00	4,07	1,82	4,03	18,24	205,66	0,09	251,61
142	60	1,50	5,78	5,10	4,38	1,55	5,02	18,78	229,99	0,08	351,00
143	60	2,20	5,94	5,08	4,16	1,67	6,09	35,76	199,05	0,18	755,04
144	60	2,10	6,14	5,71	4,68	1,80	6,80	33,31	227,06	0,15	687,96
145	60	2,19	4,68	4,05	3,31	1,38	5,07	29,10	158,21	0,18	748,19

Visser's L [cm]	s=h/L	gT^2/h	P_1 derived from v_1 [Pa]	P_2 derived from v_2 [Pa]	P_3 derived from v_3 [Pa]	ΔPa'	ΔPb'
124,50	0,90	723,19	45,80	4,56	4,31	41,24	0,26
171,87	1,21	572,90	250,17	35,84	23,58	214,33	12,26
171,89	1,20	575,28	251,00	36,07	23,96	214,93	12,12
121,85	1,39	469,81	103,89	8,36	7,26	95,53	1,10
211,65	1,08	689,70	650,27	85,20	98,59	565,07	13,39
147,30	1,33	500,44	258,81	37,35	7,73	221,47	29,62
243,44	1,37	585,95	1.377,31	133,50	223,39	1.243,80	89,89
119,47	2,23	292,87	226,25	22,44	15,66	203,81	6,77
171,82	1,94	356,83	686,16	74,37	51,13	611,79	23,25
142,48	2,38	277,74	515,84	52,72	34,89	463,12	17,83
195,50	1,40	517,62	1.147,72	156,16	71,26	991,56	84,90
300,53	1,38	661,32	2.117,18	307,04	506,55	1.810,15	199,52
162,23	2,57	265,12	1.011,64	131,65	24,49	879,99	107,16
178,70	2,90	240,98	2.006,36	189,54	61,65	1.816,82	127,90
349,64	1,81	560,14	4.137,20	308,29	911,71	3.828,91	603,42
195,38	2,16	334,27	2.731,03	227,41	165,71	2.503,62	61,70
370,79	1,71	618,71	3.693,18	559,24	1.172,61	3.133,94	613,37
211,58	2,66	281,38	4.872,28	151,53	315,91	4.720,75	164,39
183,64	1,24	568,77	535,25	62,33	31,07	472,93	31,26
195,38	1,43	505,53	1.270,70	153,14	77,50	1.117,56	75,65
263,27	1,56	539,12	2.870,43	128,50	431,70	2.741,93	303,20
241,05	2,08	382,94	3.231,31	131,77	437,03	3.099,54	305,26
412,71	1,10	1.048,09	3.527,66	403,39	1.425,11	3.124,27	1021,72
263,27	2,02	414,99	6.574,33	365,58	594,52	6.208,76	228,94
391,80	1,40	789,51	3.749,10	501,11	1.693,13	3.247,99	1192,02
218,45	3,04	249,31	6.283,19	204,24	356,08	6.078,94	151,84
117,35	0,95	696,14	21,31	8,73	18,39	12,58	9,67
179,09	0,92	717,44	111,75	30,43	67,31	81,32	36,88
225,38	0,99	706,62	216,33	93,18	243,56	123,15	150,37
150,49	1,58	411,60	128,24	48,82	97,47	79,42	48,65
261,93	1,19	624,66	503,88	128,70	457,24	375,18	328,54
117,35	2,47	267,82	97,48	47,27	78,76	50,21	31,49
206,61	1,75	389,78	427,16	152,54	359,74	274,63	207,20
144,61	2,41	270,70	218,15	96,37	159,73	121,78	63,36
327,35	1,26	660,98	886,94	200,79	887,65	686,15	686,86
167,79	2,50	262,99	421,71	147,07	293,14	274,63	146,07
284,89	1,86	416,49	852,36	268,46	978,17	583,90	709,72
259,36	1,95	379,50	928,46	236,91	1.013,40	691,55	776,48
383,44	1,34	690,93	1.166,81	385,33	1.264,61	781,48	879,27
206,61	2,61	261,62	1.047,41	287,03	637,02	760,38	349,99
407,45	1,44	667,10	1.513,64	452,41	1.933,38	1.061,23	1480,96
225,38	2,62	267,82	1.026,66	314,30	1.029,76	712,35	715,46
454,97	1,31	794,17	1.498,56	215,17	1.919,27	1.283,39	1704,10
284,89	2,30	336,97	1.089,68	465,55	1.387,88	624,14	922,33
431,29	1,38	727,95	1.744,65	329,04	2.817,65	1.415,61	2488,61
111,08	1,11	629,44	12,67	6,24	11,07	6,43	4,83
182,04	0,96	677,86	56,94	24,75	53,21	32,18	28,45
234,64	0,96	702,79	142,52	49,18	144,90	93,35	95,72
149,30	1,59	413,92	66,45	30,07	54,65	36,37	24,58
275,90	1,09	650,93	308,68	68,34	321,12	240,34	252,78
111,08	2,65	264,16	43,60	28,59	42,41	15,01	13,82
182,04	1,58	413,16	141,90	62,56	135,00	79,34	72,44

142,54	2,50	263,92	122,03	61,49	105,52	60,54	44,02
213,37	1,62	409,60	270,92	93,00	281,06	177,93	188,07
349,28	1,14	689,39	793,87	60,17	912,88	733,70	852,71
169,14	2,39	273,15	231,31	92,34	217,07	138,97	124,74
273,00	1,76	400,24	796,30	149,01	807,51	647,29	658,50
301,71	1,54	476,19	887,87	131,18	907,04	756,69	775,87
411,85	1,19	724,51	944,99	143,82	1.186,36	801,17	1042,54
213,37	2,41	274,31	620,97	149,03	577,58	471,94	428,56
438,57	1,25	713,51	1.140,42	168,60	2.012,17	971,82	1843,57
234,64	2,38	282,97	918,78	183,73	897,47	735,05	713,75
301,71	1,92	381,96	1.061,13	133,69	1.395,21	927,44	1261,51
491,33	1,21	799,39	959,92	153,73	2.055,53	806,18	1901,79
465,05	1,32	704,80	1.213,37	179,28	2.559,36	1.034,10	2380,08
488,71	0,96	1.004,82	606,70	105,44	1.422,19	501,26	1316,74